

Doctoral degree thesis

Development of UTX-121 and its derivatives as novel matrix metalloproteinase-2/9 inhibitors using celecoxib as a lead compound

(Celecoxib をリードとした新規 MMP-2/9 阻害剤
UTX-121 およびその誘導体の開発)

2022, March

Doctoral Course 2nd, Biological Science and Technology, Life and Materials Systems Engineering,
Graduate School of Advanced Technology and Science, Tokushima University

山花 啓梨

Contents

1	Abstract	1
2	Introduction	2
	2.1. Mechanisms of invasion and metastasis	2
	2.2. Extracellular matrix (ECM)	3
	2.3. Matrix metalloproteinase (MMP)	4
	2.4. Celecoxib	5
3	Materials and Methods	7
	3.1. Synthesis	7
	3.2. Cell culture	23
	3.3. <i>In vitro</i> WST-8 assay	23
	3.4. Gelatin zymography	23
	3.5. Immunofluorescence staining	24
	3.6. COX-2 inhibition assay	24
	3.7. Wound healing assay	25
	3.8. Cell invasion assay	25
4	Results	26
	4.1. Design and synthesis of UTX-121	26
	4.2. MMP inhibitory activity of UTX-121	26
	4.3. The effect of UTX-121 on cell invasion	28
	4.4. Design and synthesis of UTX-121 derivatives	28
	4.5. Antitumor activity of UTX-121 derivatives	30
	4.6. MMP-2/9 inhibitory activity of UTX-121 derivatives	30
	4.7. COX-2 inhibitory activity of UTX-121 derivatives	31
5	Discussion	35
6	Conclusion	37
	Acknowledgement	37
	References	38

1 Abstract

Matrix metalloproteinases (MMP)-2/9 are closely associated with cancer malignancy, and it has been considered that the inhibition of these MMPs may be beneficial for enhancing the antitumor and antimetastatic activities of agents. In addition, celecoxib, a COX-2 selective inhibitor, has been reported to have a poor MMPs inhibitory activity, suggesting that it is a very promising drug as an anticancer and antimetastatic agent. We have revealed that UTX-121, which was converted the sulfonamide moiety of celecoxib into a methyl ester, significantly suppressed MT1-MMP-mediated MMP-2 activation and MMP-9 production. Furthermore, UTX-121 also inhibited the migration and invasion of cancer cells. We then searched for compounds with higher MMPs inhibitory activity using a structure-activity relationship (SAR) method based on UTX-121 as a lead compound. Among them, compounds **9c** and **10c**, in which the methyl moiety of the *p*-tolyl group in UTX-121 was substituted with F and Cl, showed higher antitumor and MMPs inhibitory activities than UTX-121. These findings suggest that compounds **9c** and **10c** could be potential lead compounds for the development of potent MMPs inhibitors.

2 Introduction

2.1. Mechanisms of invasion and metastasis

Cancer cells activate a biological program called epithelial-mesenchymal transition (EMT) after proliferation in the primary lesion. EMT is an important process in which the epithelial cells are transformed into mesenchymal cells, allowing the cancer cells to gain motility [1,2]. After leaving the primary lesion, cancer cells degrade the basement membrane and invade into the connective tissue. After that, they migrate into blood vessels and lymph vessels by breaking the basement membrane, and are transported to various organs. At the metastatic lesions, cancer cells break down the basement membrane again, invade the metastatic organ, and proliferate further. This leads to the development of the metastatic lesion (Fig. 1, 2) [3]. Thus, invasion and metastasis of cancer cells are induced by the destruction of the basement membrane, the ability to degrade the basement membrane is considered to be one of the hallmarks of metastatic potential [4,5].

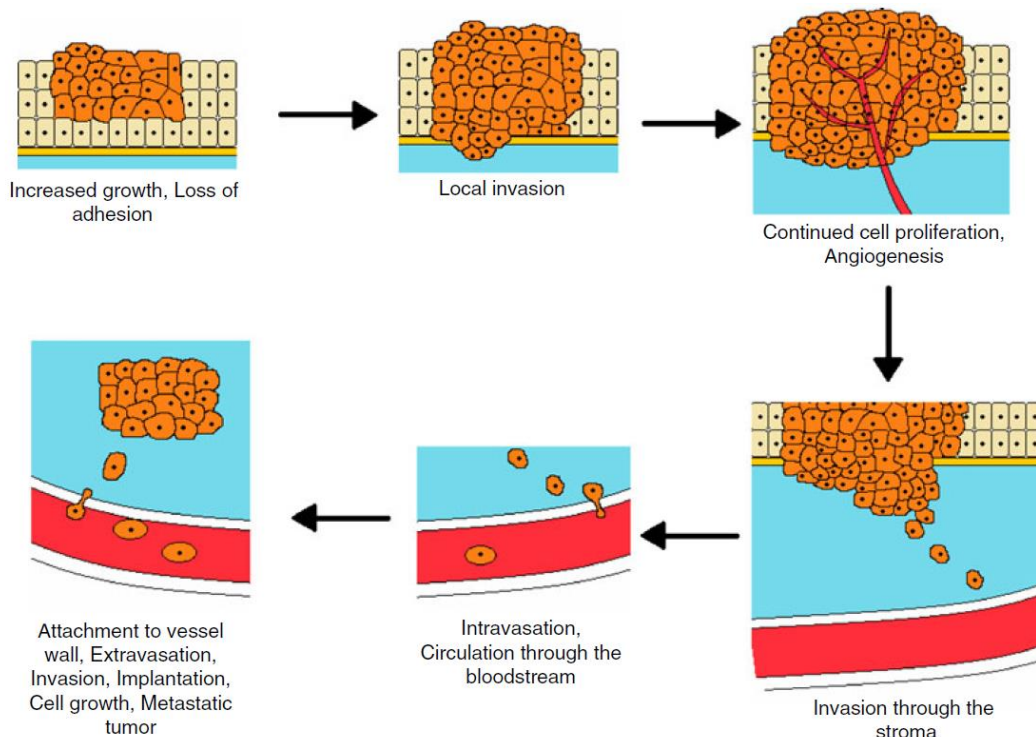


Fig. 1. Metastatic cascade. Cancer cells break down the basement membrane, invade the stroma, and are transported to various tissues through blood vessels and lymphatic vessels. (Pavese J. M. *et al.*, *Cancer Metastasis Rev.*, 2010, 29(3), 465–482.)

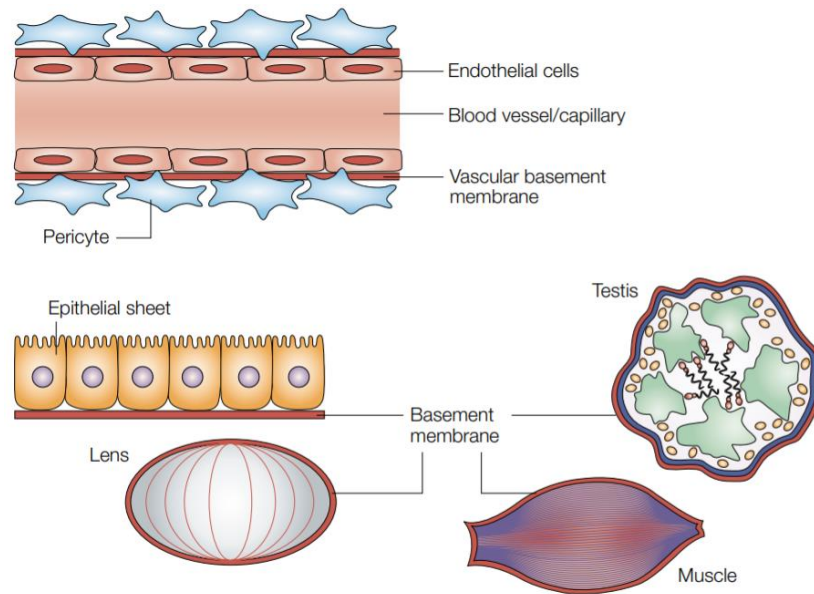


Fig. 2. Schematic of basement membrane. The basement membrane is present on the basolateral of various tissues, and forms a highly rigid sheet-like structure that divides the epithelium and the stroma. (Kalluri R., *Nat. Rev. Cancer*, **2003**, 3, 422–433.)

2.2. Extracellular matrix (ECM)

The extracellular matrix (ECM) not only acts as a physical scaffold for cells, but also plays an essential role in biological homeostasis, regulation of cell proliferation, differentiation, metabolism, migration, and apoptosis [6]. These functions are defective in cancer cells, which allows them to metastasize [7,8]. The ECM mainly consists of connective tissue and basement membrane (Fig. 3). The basement membrane is a very robust structure that lies between epithelial cells and connective tissue. It is worth emphasizing here that the tight network-like structure of the basement membrane is comprised of type IV collagen. Type IV collagen is specifically present in the basement membrane, which is significantly different from connective tissue, the latter mainly consisting of type I, II, and III collagens [9–11]. Invasion and metastasis of cancer cells are induced by the destruction of the basement membrane, indicating that the degradation of type IV collagen is a trigger for invasion and metastasis.

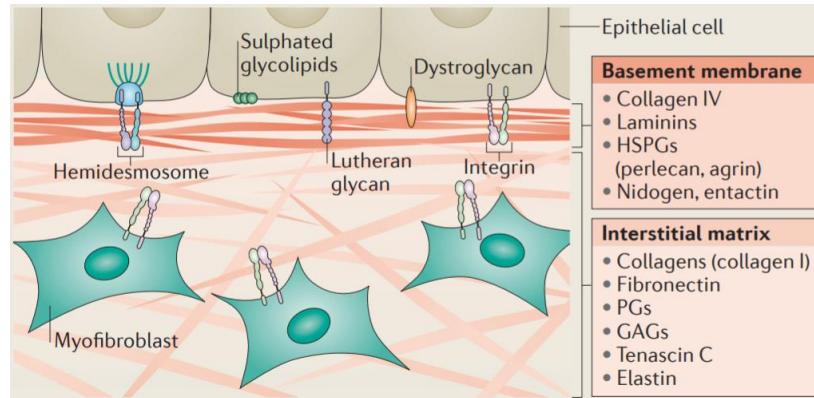


Fig. 3. Structure of ECM. ECM is composed of basement membrane and connective tissue, and type IV collagen is specifically located in the basement membrane. (Bonnans C. *et al.*, *Nat. Rev. Mol. Cell Biol.*, **2014**, *15*, 786–801.)

2.3. Matrix metalloproteinase (MMP)

Matrix metalloproteinases (MMPs) are Zn^{2+} -dependent enzymes with significant contributions to the decomposition of ECM (Fig. 4). Currently, there have been identified over 20 different subtypes of MMPs. MMPs are mainly composed of three domains: N-terminal pro-domain, catalytic domain, and C-terminal hemopexin domain. [12–14] The pro-domain is bound to the inactive MMP, and the cleavage of this domain induces the activation of MMP. The catalytic domain includes zinc ions, which are indispensable for the MMP activation. The hemopexin domain has a four propeller-like structure and is considered to be involved in the MMP substrate-specificity. Among these MMPs, we focused on MMP-2 and MMP-9. MMP-2/9 are type IV collagenases that degrade type IV collagen in the basement membrane [15]. Although their activation mechanism has not been well understood, it is suggested that MMP-2 is activated by MT1-MMP, a membrane-type MMP, which then leads to the activation of MMP-9. The degradation of type IV collagen implies the breakdown of the basement membrane, which is closely related to the invasion of cancer cells. In addition, it has been previously shown that several types of cancer overexpress these MMPs [16–19]. Therefore, we hypothesized that inhibiting these MMPs would be beneficial for antitumor and antimetastatic effects.

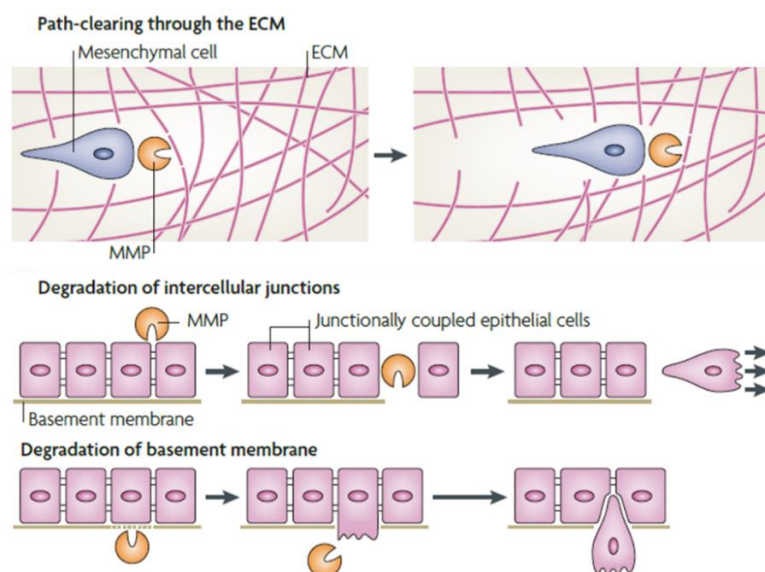


Fig. 4. Role of MMPs in metastasis. MMPs cleave ECM components such as the basement membrane to secure the migratory space for cancer cells, which leads to cancer metastasis. (Page-McCaw A. *et al.*, *Nat. Rev. Mol. Cell Biol.*, **2007**, 8, 221–233.)

2.4. Celecoxib

To develop effective antitumor and antimetastatic agents, we have focused on celecoxib (Fig. 5), a nonsteroidal anti-inflammatory drug that selectively inhibits cyclooxygenase (COX)-2 [20]. It is well known that arachidonic acid is converted into bioactive substances such as prostaglandins through a metabolic pathway called the arachidonic acid cascade, and what is necessary for this process is COX. There are two types of isozymes, COX-1 and COX-2; COX-1 is constitutively expressed in most normal cells and tissues and plays a crucial role in the regulation of biological functions. By contrast, COX-2 is derived from cytokines and inflammatory mediators accompanied by inflammation, and mainly produces prostaglandins that stimulate inflammation [21]. Therefore, celecoxib, a COX-2 selective inhibitor, has been regarded as an innovative medicine with few side effects.

In recent years, celecoxib has been found to exhibit antitumor and antimetastatic activities in various types of cancers [22–24], making it a highly valuable drug as an anticancer and antimetastatic agent. A number of studies have highlighted these activities of celecoxib, and it has been reported to have impacts on factors such as Akt, ERK, VEGF, and NF- κ B [25,26]. It has also been indicated that both COX-2-dependent and COX-2-

independent pathways are involved in this antitumor activity [25,27]. However, the underlying molecular mechanism has not yet been identified. In addition, it has been reported that celecoxib has MMPs inhibitory activity [28,29], even if it is comparatively moderate, but there are still no anticancer or antimetastatic agents based on the MMPs inhibitory effect of celecoxib.

Based on these facts, we focused on celecoxib as a hit compound for antimetastatic agents and aimed to develop novel antitumor and antimetastatic agents with potent inhibitory activities on MMP-2 and MMP-9.

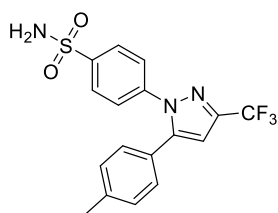


Fig. 5. Structure of celecoxib.

3 Materials and Methods

3.1. Synthesis

All reactions were carried out under a nitrogen atmosphere. Column chromatography was performed on Kanto Chemical (Tokyo, Japan) silica gel 60 N (spherical, neutral, 40–50 μm). ^1H -NMR, ^{13}C -NMR, and ^{19}F -NMR spectra were measured on JNM-ECZ400S (400 MHz) or JNM-ECA500WB (500 MHz) (JEOL, Tokyo, Japan). HRMS were recorded on a JEOL JMS-SX 102A mass spectrometer.

(Z)-1,1,1-trifluoro-4-hydroxy-4-(p-tolyl)-3-buten-2-one (1)

4'-Methylacetophenone (100 μL , 753 μmol) was dissolved in dry tetrahydrofuran (THF) (2.0 mL), and 60% sodium hydride (NaH) (65 mg, 1.63 mmol, 2.2 eq.) was added under ice-cold. After stirring for 1 h under 0 $^\circ\text{C}$, ethyl trifluoroacetate (135 μL , 1.13 mmol, 1.5 eq.) was added, and the reaction mixture was stirred for 3.5 h at room temperature. The reaction mixture was evaporated, added ice-water (5 mL), acidified to pH 6 with 1 N hydrochloric acid (HCl), and extracted 3 times with ethyl acetate (EtOAc). The organic layer was washed with water, dried over magnesium sulfate (MgSO_4), filtered, and concentrated. The residue was washed with n-hexane, and evaporated. The solid was dissolved in dichloromethane (CH_2Cl_2), and evaporated to afford **1** (140 mg, 608 μmol , 81%). ^1H -NMR (400 MHz, CDCl_3) δ : 7.86 (d, J = 8.4 Hz, 2H), 7.31 (d, J = 8.4 Hz, 2H), 6.55 (s, 1H), 2.45 (s, 3H).

4-(5-(p-Tolyl)-3-(trifluoromethyl)-1H-pyrazol-1-yl)benzoic acid (2)

4-Hydrazinobenzoic acid (361 mg, 2.37 mmol, 1.1 eq.) was dissolved in dry ethanol (EtOH) (30 mL), added 2 N HCl (1.3 mL) and **1** (503 mg, 2.19 mol). After stirring for 0.5 h at 75 $^\circ\text{C}$, the reaction mixture was extracted two times with EtOAc, and washed with brine. The organic layer was dried over MgSO_4 , filtered, and concentrated to afford **2** (741 mg, 2.14 mmol, 98%). ^1H -NMR (400 MHz, $(\text{CD}_3)_2\text{CO}$) δ : 8.10 (d, J = 8.8 Hz, 2H), 7.51 (d, J = 8.8 Hz, 2H), 7.24 (s, 4H), 7.00 (s, 1H), 2.35 (s, 3H).

Methyl 4-(5-(4-methylphenyl)-3-(trifluoromethyl)-1H-pyrazol-1-yl) benzoate (UTX-121)

2 (53 mg, 153 μmol) was dissolved in dry methanol (MeOH) (1.5 mL), and added thionyl chloride (SOCl_2) (55 μL , 763 μL , 5.0 eq.) under ice-cold. After stirring for 19.5 h at room temperature, the reaction mixture was quenched with aqueous saturated sodium hydrogen carbonate (NaHCO_3), and evaporated. The residue was extracted two times with EtOAc and washed with brine. The organic layer was dried over MgSO_4 , filtered, and concentrated. The residue was purified by silica gel flash column chromatography (n-hexane/EtOAc = 3:1) to afford UTX-121 (35 mg, 97.1 μmol , 63.5%). $^1\text{H-NMR}$ (400 MHz, $(\text{CD}_3)_2\text{CO}$) δ : 8.07 (d, $J = 8.8$ Hz, 2H), 7.51 (d, $J = 8.8$ Hz, 2H), 7.23 (brs, 4H), 6.99 (s, 1H), 3.91 (s, 3H), 2.35 (s, 3H); HRMS (ESI-TOF): m/z calcd. for $\text{C}_{19}\text{H}_{15}\text{F}_3\text{N}_2\text{O}_2$ $[\text{M} + \text{H}]^+$ 361.1164, found 361.1166.

(4-(5-(*p*-Tolyl)-3-(trifluoromethyl)-1H-pyrazol-1-yl)phenyl)methanol (3)

Lithium aluminum hydride in THF (200 μL , 200 μmol , 1.4 eq.) was slowly added to dry THF (500 μL), and **2** (in 1.5 mL THF) (51 mg, 147 μmol) was added under ice-cold. After stirring for 0.5 h at 0 $^\circ\text{C}$, the reaction mixture was stirred for 1.5 h at room temperature. The reaction mixture was quenched with RO water and 15% sodium hydroxide (NaOH) aq., filtered with celite, and concentrated. The residue was purified by silica gel column chromatography (CH_2Cl_2 only) to afford **3** (37 mg, 111 μmol , 76%). $^1\text{H-NMR}$ (400 MHz, CDCl_3) δ : 7.36 (d, $J = 8.0$ Hz, 2H), 7.31 (d, $J = 8.8$ Hz, 2H), 7.12 (q, $J = 8.8, 12.4$ Hz, 4H), 6.72 (s, 1H), 4.73 (d, $J = 6.0$ Hz, 2H), 2.35 (s, 3H); HRMS (ESI-TOF): m/z calcd. for $\text{C}_{18}\text{H}_{16}\text{F}_3\text{N}_2\text{O}$ $[\text{M} + \text{H}]^+$ 333.1215, found 333.1196.

1-(4-(Methoxymethyl)phenyl)-5-(*p*-tolyl)-3-(trifluoromethyl)-1H-pyrazole (4)

60% NaH (23 mg, 575 μmol , 3.3 eq.) was dissolved in dry THF (2.0 mL), and **3** (in 2.0 mL THF) (57 mg, 172 μmol) was added on ice bath. After stirring for 1.5 h on ice bath, methyl iodide (32.2 μL , 517 μmol , 3.0 eq.) was added. After stirring for 19 h at room temperature, the reaction mixture was quenched with DI water (1.0 mL), extracted two times with EtOAc, and washed with brine. The organic layer was dried over MgSO_4 , filtered, and concentrated. The residue was purified by silica gel flash column chromatography (n-

hexane/EtOAc = 10:1) to afford **4** (38 mg, 110 μ mol, 64%). $^1\text{H-NMR}$ (400 MHz, CDCl_3) δ : 7.31 (q, $J = 8.4$, 15.6 Hz, 4H), 7.11 (q, $J = 8.8$, 10.4 Hz, 4H), 6.71 (s, 1H), 4.47 (s, 2H), 3.40 (s, 3H), 2.35 (s, 3H); HRMS (ESI-TOF): m/z calcd. for $\text{C}_{19}\text{H}_{18}\text{F}_3\text{N}_2\text{O}$ $[\text{M} + \text{H}]^+$ 347.1371, found 347.1387.

Ethyl 4-(5-(*p*-tolyl)-3-(trifluoromethyl)-1*H*-pyrazol-1-yl)benzoate (5)

2 (50 mg, 144 μ mol) was dissolved in dry EtOH, and added SOCl_2 (52.0 μL , 721 μ mol, 5.0 eq.) under ice-cold. After stirring for 24 h at room temperature, the reaction mixture was quenched with sat. NaHCO_3 aq. (1.5 mL), and evaporated. The residue was extracted two times with EtOAc, and washed with brine. The organic layer was dried over MgSO_4 , filtered, and concentrated. The residue was purified by silica gel flash column chromatography (n-hexane/EtOAc = 10:1) to afford **5** (20 mg, 53.4 μ mol, 37%). $^1\text{H-NMR}$ (400 MHz, CDCl_3) δ : 8.04 (d, $J = 7.2$ Hz, 2H), 7.39 (d, $J = 7.2$ Hz, 2H), 7.13 (q, $J = 8.0$, 19.2 Hz, 4H), 6.73 (s, 1H), 4.38 (q, $J = 7.2$, 14.4 Hz, 2H), 2.37 (s, 3H), 1.40 (t, $J = 7.2$ Hz, 3H); HRMS (ESI-TOF): m/z calcd. for $\text{C}_{20}\text{H}_{18}\text{F}_3\text{N}_2\text{O}_2$ $[\text{M} + \text{H}]^+$ 375.1320, found 375.1328.

Propyl 4-(5-(*p*-tolyl)-3-(trifluoromethyl)-1*H*-pyrazol-1-yl)benzoate (6)

The title compound was synthesized from **2** (51 mg, 147 μ mol) in 68% yield using the method described for the preparation of **5**. 1-Propanol was used as a solvent instead of EtOH. $^1\text{H-NMR}$ (400 MHz, CDCl_3) δ : 8.03 (d, $J = 8.8$ Hz, 2H), 7.39 (d, $J = 8.8$ Hz, 2H), 7.13 (q, $J = 8.4$, 20.4 Hz, 4H), 6.73 (s, 1H), 4.28 (t, $J = 7.2$ Hz, 2H), 2.37 (s, 3H), 1.85–1.75 (m, 2H), 1.03 (t, $J = 7.2$ Hz, 3H); HRMS (ESI-TOF): m/z calcd. for $\text{C}_{21}\text{H}_{20}\text{F}_3\text{N}_2\text{O}_2$ $[\text{M} + \text{H}]^+$ 389.1477, found 389.1481.

Isopropyl 4-(5-(*p*-tolyl)-3-(trifluoromethyl)-1*H*-pyrazol-1-yl)benzoate (7)

The title compound was synthesized from **2** (52 mg, 150 μ mol) in 22% yield using the method described for the preparation of **5**. 2-Propanol was used as a solvent instead of EtOH. $^1\text{H-NMR}$ (400 MHz, CDCl_3) δ : 8.02 (d, $J = 8.8$ Hz, 2H), 7.38 (d, $J = 8.8$ Hz, 2H), 7.12 (q, $J = 8.0$, 20.8 Hz, 4H), 6.73 (s, 1H), 5.30–5.20 (m, 1H), 2.37 (s, 3H), 1.37 (d, $J = 6.4$ Hz, 6H); HRMS (ESI-TOF): m/z calcd. for $\text{C}_{21}\text{H}_{20}\text{F}_3\text{N}_2\text{O}_2$ $[\text{M} + \text{H}]^+$

389.1477, found 389.1484.

***tert*-Butyl 4-(5-(*p*-tolyl)-3-(trifluoromethyl)-1*H*-pyrazol-1-yl)benzoate (8)**

2 (50 mg, 144 μ mol), benzyltriethylammonium chloride (36 mg, 158 μ mol, 1.1 eq.) and potassium carbonate (K_2CO_3) (496 mg, 3.59 mmol, 25 eq.) were dissolved in *N,N*-dimethylacetamide (1.0 mL), and added 2-bromo-2-methylpropane (723 μ L, 6.48 mmol, 45 eq.). After stirring for 19 h at 55 $^\circ$ C, the reaction mixture was extracted two times with EtOAc, and washed with brine. The organic layer was dried over $MgSO_4$, filtered, and concentrated. The residue was purified by silica gel flash column chromatography (n-hexane/EtOAc = 4:1) to afford **8** (52 mg, 129 μ mol, 90%). 1H -NMR (400 MHz, CD_3OD) δ : 7.99 (d, J = 8.0 Hz, 2H), 7.40 (d, J = 8.8 Hz, 2H), 7.18 (q, J = 8.0, 18.4 Hz, 4H), 6.91 (s, 1H), 2.35 (s, 3H), 1.60 (s, 9H); HRMS (ESI-TOF): m/z calcd. for $C_{22}H_{22}F_3N_2O_2$ [$M + H$] $^+$ 403.1633, found 403.1615.

Methyl 4-(5-(4-fluorophenyl)-3-(trifluoromethyl)-1*H*-pyrazol-1-yl)benzoate (9c)

4'-Fluoroacetophenone (300 μ L, 2.48 mmol) was dissolved in dry THF (6.0 mL) under ice-cold, and 60% NaH (223 mg, 5.58 mmol, 2.3 eq.) was added. After stirring for 1 h under 0 $^\circ$ C, ethyl trifluoroacetate (444 μ L, 3.72 mmol, 1.5 eq.) was added, and the reaction mixture was stirred for 1 h at room temperature. The reaction mixture was acidified to pH 6 with 1 N HCl, extracted two times with EtOAc, and washed with brine. The organic layer was dried over $MgSO_4$, filtered, and concentrated. The residue was reprecipitated with EtOAc and n-hexane to afford (*Z*)-1,1,1-trifluoro-4-(4-fluorophenyl)-4-hydroxy-3-buten-2-one (**9a**) (373 mg, 1.59 mmol, 64%). 1H -NMR (400 MHz, $(CD_3)_2CO$) δ : 8.00 (t, J = 7.2 Hz, 2H), 7.14 (t, J = 8.8 Hz, 2H), 6.23 (s, 1H).

4-(5-(4-Fluorophenyl)-3-(trifluoromethyl)-1*H*-pyrazol-1-yl)benzoic acid (**9b**) was synthesized from **9a** (196 mg, 837 μ mol) in 94% yield using the method described for the preparation of **2**. 1H -NMR (400 MHz, $(CD_3)_2CO$) δ : 8.11 (d, J = 9.2 Hz, 2H), 7.52 (d, J = 8.4 Hz, 2H), 7.43 (q, J = 4.8, 8.4 Hz, 2H), 7.21 (t, J = 8.8 Hz, 2H), 7.05 (s, 1H).

9c was synthesized from **9b** (316 mg, 902 μ mol) in 60% yield using the method described for the preparation of UTX-121. 1H -NMR (400 MHz, $CDCl_3$) δ : 8.04 (d, J = 6.8 Hz, 2H), 7.38 (d, J = 6.8 Hz, 2H), 7.20

(t, $J = 7.2$ Hz, 2H), 7.05 (t, $J = 7.8$ Hz, 2H), 6.75 (s, 1H), 3.93 (s, 3H); ^{13}C -NMR (126 MHz, CDCl_3) δ : 166.1, 163.3 (d, $^1J_{\text{CF}} = 251$ Hz), 144.1, 144.0 (q, $^2J_{\text{CF}} = 38.4$ Hz), 142.6, 130.9 (d, $^3J_{\text{CF}} = 8.4$ Hz), 130.7, 130.1, 125.2, 125.1, 121.2 (q, $^1J_{\text{CF}} = 269$ Hz), 116.3 (d, $^2J_{\text{CF}} = 21.7$ Hz), 106.4, 52.5; ^{19}F -NMR (373 MHz, CDCl_3) δ : -62.3, -110.6; HRMS (ESI-TOF): m/z calcd. for $\text{C}_{18}\text{H}_{13}\text{F}_4\text{N}_2\text{O}_2$ $[\text{M} + \text{H}]^+$ 365.0913, found 365.0915.

Methyl 4-(5-(4-chlorophenyl)-3-(trifluoromethyl)-1H-pyrazol-1-yl)benzoate (10c)

(*Z*)-4-(4-chlorophenyl)-1,1,1-trifluoro-4-hydroxy-3-buten-2-one (**10a**) was synthesized from 4'-chloroacetophenone (500 μL , 3.85 mmol) in 53% yield using the method described for the preparation of **9a**. ^1H -NMR (400 MHz, $(\text{CD}_3)_2\text{CO}$) δ : 7.89 (d, $J = 8.4$ Hz, 2H), 7.49 (d, $J = 8.8$ Hz, 2H), 6.54 (s, 1H).

4-(5-(4-Chlorophenyl)-3-(trifluoromethyl)-1H-pyrazol-1-yl)benzoic acid (**10b**) was synthesized from **10a** (404 mg, 1.61 mmol) in 64% yield using the method described for the preparation of **2**. ^1H -NMR (400 MHz, $(\text{CD}_3)_2\text{CO}$) δ : 8.12 (d, $J = 8.8$ Hz, 2H), 7.53 (d, $J = 8.8$ Hz, 2H), 7.47 (d, $J = 8.4$ Hz, 2H), 7.40 (d, $J = 8.8$ Hz, 2H), 7.10 (s, 1H).

10c was synthesized from **10b** (152 mg, 414 μmol) in 72% yield using the method described for the preparation of UTX-121. ^1H -NMR (400 MHz, CDCl_3) δ : 8.05 (d, $J = 9.2$ Hz, 2H), 7.38 (d, $J = 8.8$ Hz, 2H), 7.33 (d, $J = 8.4$ Hz, 2H), 7.15 (d, $J = 8.4$ Hz, 2H), 6.77 (s, 1H), 3.93 (s, 3H); ^{13}C -NMR (126 MHz, CDCl_3) δ : 166.1, 144.1 (q, $^2J_{\text{CF}} = 38.4$ Hz), 143.9, 142.5, 135.8, 130.8, 130.2, 129.4, 127.4, 125.2, 125.1, 121.1 (q, $^1J_{\text{CF}} = 269$ Hz), 106.5, 52.6; ^{19}F -NMR (471 MHz, CDCl_3) δ : -62.3; HRMS (ESI-TOF): m/z calcd. for $\text{C}_{18}\text{H}_{13}\text{ClF}_3\text{N}_2\text{O}_2$ $[\text{M} + \text{H}]^+$ 381.0618, found 381.0642.

Methyl 4-(5-(4-bromophenyl)-3-(trifluoromethyl)-1H-pyrazol-1-yl)benzoate (11c)

4'-Bromoacetophenone (302 mg, 1.52 mmol) was dissolved in dry THF (4.0 mL), and 60% NaH (85 mg, 2.13 mmol, 1.4 eq.) was added under ice-cold. After stirring for 1 h under 0 $^\circ\text{C}$, ethyl trifluoroacetate (267 μL , 2.24 mmol, 1.5 eq.) was added, and the reaction mixture was stirred for 0.5 h at room temperature. The reaction mixture was acidified to pH 6 with 1 N HCl, extracted two times with EtOAc, and washed with brine to afford (*Z*)-4-(4-bromophenyl)-1,1,1-trifluoro-4-hydroxy-3-buten-2-one (**11a**) (343 mg, 1.16 mmol, 76%). ^1H -

NMR (400 MHz, (CD₃)₂CO) δ : 7.84 (d, J = 8.4 Hz, 2H), 7.55 (d, J = 8.8 Hz, 2H), 6.26 (s, 1H).

4-(5-(4-Bromophenyl)-3-(trifluoromethyl)-1*H*-pyrazol-1-yl)benzoic acid (**11b**) was synthesized from **11a** (153 mg, 519 μ mol) in 90% yield using the method described for the preparation of **2**. ¹H-NMR (400 MHz, (CD₃)₂CO) δ : 8.12 (d, J = 9.2 Hz, 2H), 7.62 (d, J = 8.8 Hz, 2H), 7.54 (d, J = 8.8 Hz, 2H), 7.33 (d, J = 8.8 Hz, 2H), 7.10 (s, 1H).

11c was synthesized from **11b** (104 mg, 252 μ mol) in 54% yield using the method described for the preparation of UTX-121. ¹H-NMR (400 MHz, (CD₃)₂CO) δ : 8.09 (d, J = 8.8 Hz, 2H), 7.61 (d, J = 8.4 Hz, 2H), 7.54 (d, J = 9.2 Hz, 2H), 7.32 (d, J = 8.8 Hz, 2H), 7.10 (s, 1H), 3.91 (s, 3H); HRMS (ESI-TOF): m/z calcd. for C₁₈H₁₃BrF₃N₂O₂ [M + H]⁺ 425.0113, found 425.2155.

Methyl 4-(5-phenyl-3-(trifluoromethyl)-1*H*-pyrazol-1-yl)benzoate (12c)

(*Z*)-1,1,1-trifluoro-4-hydroxy-4-phenyl-3-buten-2-one (**12a**) was synthesized from acetophenone (1.00 mL, 8.57 mmol) quantitatively using the method described for the preparation of **11a**. ¹H-NMR (400 MHz, (CD₃)₂CO) δ : 7.95 (d, J = 7.2 Hz, 2H), 7.50 (t, J = 7.6 Hz, 1H), 7.42 (t, J = 8.0 Hz, 2H), 6.35 (s, 1H).

4-(5-Phenyl-3-(trifluoromethyl)-1*H*-pyrazol-1-yl)benzoic acid (**12b**) was synthesized from **12a** (395 mg, 1.83 mmol) in 95% yield using the method described for the preparation of **2**. ¹H-NMR (400 MHz, (CD₃)₂CO) δ : 8.09 (d, J = 8.4 Hz, 2H), 7.51 (d, J = 8.8 Hz, 2H), 7.45–7.35 (m, 5H), 7.04 (s, 1H).

12c was synthesized from **12b** (97 mg, 292 μ mol) in 52% yield using the method described for the preparation of UTX-121. ¹H-NMR (400 MHz, CDCl₃) δ : 8.03 (d, J = 8.8 Hz, 2H), 7.41–7.32 (m, 5H), 7.22 (d, J = 6.4 Hz, 2H), 6.77 (s, 1H), 3.92 (s, 3H); HRMS (ESI-TOF): m/z calcd. for C₁₈H₁₄F₃N₂O₂ [M + H]⁺ 347.1007, found 347.1004.

Methyl 4-(5-(4-ethylphenyl)-3-(trifluoromethyl)-1*H*-pyrazol-1-yl)benzoate (13c)

60% NaH (166 mg, 4.15 mmol, 2.1 eq.) was dissolved in dry *tert*-butyl methyl ether (6.0 mL), and added *p*-ethylacetophenone (300 μ L, 2.01 mmol) under ice-cold. After stirring for 1 h under 0 °C, ethyl trifluoroacetate (361 μ L, 3.02 mmol, 1.5 eq.) was added, and the reaction mixture was stirred for 2.5 h at room

temperature. The reaction mixture was acidified to pH 6 with 1 N HCl, extracted two times with EtOAc, and washed with brine. The organic layer was dried over MgSO₄, filtered, and concentrated. The residue was reprecipitated with EtOAc and n-hexane to afford (*Z*)-4-(4-ethylphenyl)-1,1,1-trifluoro-4-hydroxy-3-buten-2-one (**13a**) (193 mg, 790 μmol, 39%). ¹H-NMR (400 MHz, (CD₃)₂CO) δ: 7.91 (d, *J* = 8.4 Hz, 2H), 7.30 (d, *J* = 7.6 Hz, 2H), 6.36 (s, 1H), 2.68 (q, *J* = 7.6, 15.2 Hz, 2H), 1.22 (t, *J* = 7.6 Hz, 3H).

4-Hydrazinobenzoic acid (69 mg, 453 μmol, 1.1 eq.) was dissolved in dry EtOH (5.0 mL), added 2 N HCl (260 μL) and **13a** (99 mg, 405 μmol). After stirring for 1.5 h at 75 °C, the reaction mixture was extracted two times with EtOAc, and washed with brine. The organic layer was dried over MgSO₄, filtered, and concentrated. The residue was dissolved in EtOAc, and n-hexane was added to remove the precipitated solid by filtration. The filtrate was evaporated to afford 4-(5-(4-Ethylphenyl)-3-(trifluoromethyl)-1*H*-pyrazol-1-yl)benzoic acid (**13b**) (118 mg, 328 μmol, 81%). ¹H-NMR (400 MHz, CD₃OD) δ: 8.05 (d, *J* = 8.8 Hz, 2H), 7.42 (d, *J* = 8.8 Hz, 2H), 7.21 (q, *J* = 8.8, 14.8 Hz, 4H), 6.91 (s, 1H), 2.66 (q, *J* = 7.6, 15.2 Hz, 2H), 1.22 (t, *J* = 7.6 Hz, 3H).

13b (90 mg, 250 μmol) was dissolved in dry MeOH, and added SOCl₂ (90.0 μL, 1.25 mmol, 5.0 eq.) under ice-cold. After stirring for 23 h at room temperature, the reaction mixture was quenched with sat. NaHCO₃ aq., extracted two times with EtOAc, and washed with brine. The organic layer was dried over MgSO₄, filtered, and concentrated. The residue was purified by silica gel flash column chromatography (n-hexane/EtOAc = 10:1) to afford **13c** (57 mg, 152 μmol, 61%). ¹H-NMR (400 MHz, CDCl₃) δ: 8.03 (d, *J* = 8.8 Hz, 2H), 7.40 (d, *J* = 8.4 Hz, 2H), 7.15 (q, *J* = 8.0, 19.6 Hz, 4H), 6.74 (s, 1H), 3.93 (s, 3H), 2.66 (q, *J* = 8.0, 15.2 Hz, 2H), 1.25 (t, *J* = 7.6 Hz, 3H); HRMS (ESI-TOF): *m/z* calcd. for C₂₀H₁₈F₃N₂O₂ [M + H]⁺ 375.1320, found 375.1323.

Methyl 4-(3-(trifluoromethyl)-5-(4-(trifluoromethyl)phenyl)-1*H*-pyrazol-1-yl)benzoate (14c)

(*Z*)-1,1,1-trifluoro-4-hydroxy-4-(4-(trifluoromethyl)phenyl)-3-buten-2-one (**14a**) was synthesized from 4'-(trifluoromethyl)acetophenone (200 μL, 982 μmol) in 72% yield using the method described for the preparation of **13a**. ¹H-NMR (400 MHz, (CD₃)₂CO) δ: 8.18 (d, *J* = 8.0 Hz, 2H), 7.80 (d, *J* = 8.8 Hz, 2H), 6.42 (s, 1H).

4-Hydrazinobenzoic acid (112 mg, 736 μmol , 1.2 eq.) was dissolved in dry EtOH (5.0 mL), added 2 N HCl (450 μL) and **14a** (180 mg, 633 μmol). After stirring for 2 h at 75 $^{\circ}\text{C}$, the reaction mixture was extracted two times with EtOAc, and washed with brine. The organic layer was dried over MgSO_4 , filtered, and concentrated. The residue was reprecipitated with EtOAc and n-hexane to afford 4-(3-(Trifluoromethyl)-5-(4-(trifluoromethyl)phenyl)-1H-pyrazol-1-yl)benzoic acid (**14b**) (168 mg, 420 μmol , 66%). $^1\text{H-NMR}$ (400 MHz, $(\text{CD}_3)_2\text{CO}$) δ : 8.12 (d, $J = 8.4$ Hz, 2H), 7.78 (d, $J = 8.4$ Hz, 2H), 7.62 (d, $J = 8.0$ Hz, 2H), 7.53 (d, $J = 8.4$ Hz, 2H), 7.20 (s, 1H).

14c was synthesized from **14b** (115 mg, 317 μmol) in 68% yield using the method described for the preparation of UTX-121. $^1\text{H-NMR}$ (400 MHz, CDCl_3) δ : 8.07 (d, $J = 8.4$ Hz, 2H), 7.62 (d, $J = 8.8$ Hz, 2H), 7.38 (d, $J = 8.8$ Hz, 2H), 7.35 (d, $J = 8.4$ Hz, 2H), 6.84 (s, 1H), 3.94 (s, 3H); HRMS (ESI-TOF): m/z calcd. for $\text{C}_{19}\text{H}_{13}\text{F}_6\text{N}_2\text{O}_2$ $[\text{M} + \text{H}]^+$ 415.0881, found 415.0997.

Methyl 4-(5-(4-cyanophenyl)-3-(trifluoromethyl)-1H-pyrazol-1-yl)benzoate (**15c**)

(*Z*)-4-(4,4,4-trifluoro-1-hydroxy-3-oxo-1-buten-1-yl)benzotrile (**15a**) was synthesized from 4-acetylbenzotrile (200 mg, 1.38 mmol) in 92% yield using the method described for the preparation of **13a**. $^1\text{H-NMR}$ (400 MHz, $(\text{CD}_3)_2\text{CO}$) δ : 8.15 (d, $J = 8.0$ Hz, 2H), 7.87 (d, $J = 8.4$ Hz, 2H), 6.42 (s, 1H).

4-(5-(4-Cyanophenyl)-3-(trifluoromethyl)-1H-pyrazol-1-yl)benzoic acid (**15b**) was synthesized from **15a** (145 mg, 601 μmol) in 61% yield using the method described for the preparation of **2**. $^1\text{H-NMR}$ (400 MHz, CD_3OD) δ : 8.09 (d, $J = 8.4$ Hz, 2H), 7.75 (d, $J = 8.0$ Hz, 2H), 7.48 (d, $J = 8.4$ Hz, 2H), 7.44 (d, $J = 8.4$ Hz, 2H), 7.12 (s, 1H).

15c was synthesized from **15b** (110 mg, 308 μmol) in 56% yield using the method described for the preparation of **13c**. $^1\text{H-NMR}$ (400 MHz, CDCl_3) δ : 8.08 (d, $J = 8.4$ Hz, 2H), 7.65 (d, $J = 8.8$ Hz, 2H), 7.36 (q, $J = 8.8, 12.0$ Hz, 4H), 6.86 (s, 1H), 3.94 (s, 3H); HRMS (ESI-TOF): m/z calcd. for $\text{C}_{19}\text{H}_{13}\text{F}_3\text{N}_3\text{O}_2$ $[\text{M} + \text{H}]^+$ 372.0960, found 372.0980.

Methyl 4-(5-(4-(methylthio)phenyl)-3-(trifluoromethyl)-1*H*-pyrazol-1-yl)benzoate (**16c**)

(*Z*)-1,1,1-trifluoro-4-hydroxy-4-(4-(methylthio)phenyl)-3-buten-2-one (**16a**) was synthesized from 4-(methylthio)acetophenone (100 mg, 602 μ mol) in 30% yield using the method described for the preparation of **11a**. ¹H-NMR (400 MHz, (CD₃)₂CO) δ : 8.07 (d, *J* = 8.8 Hz, 2H), 7.43 (d, *J* = 8.4 Hz, 2H), 6.88 (s, 1H), 2.60 (s, 3H).

4-(5-(4-(Methylthio)phenyl)-3-(trifluoromethyl)-1*H*-pyrazol-1-yl)benzoic acid (**16b**) was synthesized from **16a** (36 mg, 137 μ mol) in 73% yield using the method described for the preparation of **2**. ¹H-NMR (400 MHz, CD₃OD) δ : 8.07 (d, *J* = 7.2 Hz, 2H), 7.43 (d, *J* = 8.0 Hz, 2H), 7.22 (q, *J* = 8.8, 17.6 Hz, 4H), 6.94 (s, 1H), 2.48 (s, 3H).

16c was synthesized from **16b** (36 mg, 95.1 μ mol) in 53% yield using the method described for the preparation of UTX-121. ¹H-NMR (400 MHz, CDCl₃) δ : 8.03 (d, *J* = 9.2 Hz, 2H), 7.39 (d, *J* = 8.8 Hz, 2H), 7.17 (d, *J* = 8.4, 2H), 7.11 (d, *J* = 8.4, 2H), 6.73 (s, 1H), 3.92 (s, 3H), 2.48 (s, 3H); HRMS (ESI-TOF): *m/z* calcd. for C₁₉H₁₆F₃N₂O₂S [M + H]⁺ 393.0885, found 393.0850.

Methyl 4-(5-(4-hydroxyphenyl)-3-(trifluoromethyl)-1*H*-pyrazol-1-yl)benzoate (**17c**)

(*Z*)-1,1,1-trifluoro-4-hydroxy-4-(4-hydroxyphenyl)-3-buten-2-one (**17a**) was synthesized from *p*-hydroxyacetophenone (204 mg, 1.50 mmol) in 15% yield using the method described for the preparation of **13a**. ¹H-NMR (400 MHz, (CD₃)₂CO) δ : 9.34 (brs, 1H), 7.95 (d, *J* = 8.8 Hz, 2H), 6.92 (d, *J* = 8.8 Hz, 2H).

4-Hydrazinobenzoic acid (44 mg, 289 μ mol, 1.6 eq.) was dissolved in dry EtOH (3.0 mL), added 2 N HCl (130 μ L) and **17a** (43 mg, 185 μ mol). After stirring for 3 h at 75 °C, EtOAc was added and the precipitate was removed by filtration. The filtrate was evaporated, and the residue was reprecipitated with EtOAc and *n*-hexane to afford 4-(5-(4-Hydroxyphenyl)-3-(trifluoromethyl)-1*H*-pyrazol-1-yl)benzoic acid (**17b**) (21 mg, 60.3 μ mol, 33%). ¹H-NMR (400 MHz, CD₃OD) δ : 8.06 (d, *J* = 8.4 Hz, 2H), 7.42 (d, *J* = 8.4 Hz, 2H), 7.10 (d, *J* = 8.8 Hz, 2H), 6.84 (s, 1H), 6.77 (d, *J* = 8.4 Hz, 2H).

17c was synthesized from **17b** (20 mg, 57.4 μ mol) in 66% yield using the method described for the preparation of **13c**. ¹H-NMR (400 MHz, CDCl₃) δ : 8.03 (d, *J* = 8.4 Hz, 2H), 7.40 (d, *J* = 8.4 Hz, 2H), 7.09 (d, *J*

= 8.4 Hz, 2H), 6.80 (d, $J = 8.0$ Hz, 2H), 6.71 (s, 1H), 3.93 (s, 3H); HRMS (ESI-TOF): m/z calcd. for $C_{18}H_{14}F_3N_2O_3$ $[M + H]^+$ 363.0956, found 363.0976.

Methyl 4-(5-(4-methoxyphenyl)-3-(trifluoromethyl)-1H-pyrazol-1-yl)benzoate (18c)

(*Z*)-1,1,1-trifluoro-4-hydroxy-4-(4-methoxyphenyl)-3-buten-2-one (**18a**) was synthesized from 4'-methoxyacetophenone (105 mg, 699 μ mol) in 89% yield using the method described for the preparation of **13a**. 1H -NMR (400 MHz, $(CD_3)_2CO$) δ : 7.97 (d, $J = 8.8$ Hz, 2H), 6.98 (d, $J = 9.2$ Hz, 2H), 6.33 (s, 1H), 3.86 (s, 3H).

4-(5-(4-Methoxyphenyl)-3-(trifluoromethyl)-1*H*-pyrazol-1-yl)benzoic acid (**18b**) was synthesized from **18a** (127 mg, 516 μ mol) in 71% yield using the method described for the preparation of **13b**. 1H -NMR (400 MHz, CD_3OD) δ : 8.06 (d, $J = 8.8$ Hz, 2H), 7.43 (d, $J = 8.4$ Hz, 2H), 7.20 (d, $J = 9.2$ Hz, 2H), 6.92 (d, $J = 8.4$ Hz, 2H), 6.88 (s, 1H), 3.80 (s, 3H).

18c was synthesized from **18b** (115 mg, 317 μ mol) in 68% yield using the method described for the preparation of UTX-121. 1H -NMR (400 MHz, $CDDl_3$) δ : 8.03 (d, $J = 8.0$ Hz, 2H), 7.40 (d, $J = 8.8$ Hz, 2H), 7.14 (d, $J = 8.8$ Hz, 2H), 6.86 (d, $J = 9.2$ Hz, 2H), 6.71 (s, 1H), 3.93 (s, 3H), 3.82 (s, 3H); HRMS (ESI-TOF): m/z calcd. for $C_{19}H_{16}F_3N_2O_3$ $[M + H]^+$ 377.1113, found 377.1113.

Methyl 4-(5-(4-nitrophenyl)-3-(trifluoromethyl)-1H-pyrazol-1-yl)benzoate (19c)

(*Z*)-1,1,1-trifluoro-4-hydroxy-4-(4-nitrophenyl)-3-buten-2-one (**19a**) was synthesized from 4'-nitroacetophenone (211 mg, 1.28 mmol) in 94% yield using the method described for the preparation of **13a**. 1H -NMR (400 MHz, $(CD_3)_2CO$) δ : 8.25 (d, $J = 8.8$ Hz, 2H), 8.15 (d, $J = 8.4$ Hz, 2H), 6.33 (s, 1H).

4-(5-(4-Nitrophenyl)-3-(trifluoromethyl)-1*H*-pyrazol-1-yl)benzoic acid (**19b**) was synthesized from **19a** (182 mg, 697 μ mol) in 90% yield using the method described for the preparation of **14b**. 1H -NMR (400 MHz, CD_3OD) δ : 8.24 (d, $J = 9.2$ Hz, 2H), 8.08 (d, $J = 8.8$ Hz, 2H), 7.55 (d, $J = 9.2$ Hz, 2H), 7.45 (d, $J = 8.4$ Hz, 2H), 7.16 (s, 1H).

19c was synthesized from **19b** (185 mg, 490 μ mol) in 46% yield using the method described for the preparation of UTX-121. 1H -NMR (400 MHz, $CDCl_3$) δ : 8.22 (d, $J = 8.8$ Hz, 2H), 8.08 (d, $J = 8.8$ Hz, 2H), 7.40

(q, $J = 8.8, 11.6$ Hz, 4H), 6.90 (s, 1H), 3.94 (s, 3H); HRMS (ESI-TOF): m/z calcd. for $C_{18}H_{13}F_3N_3O_4$ $[M + H]^+$ 392.0858, found 392.0880.

Methyl 4-(5-(4-(methylamino)phenyl)-3-(trifluoromethyl)-1H-pyrazol-1-yl)benzoate (20c)

(*Z*)-1,1,1-trifluoro-4-hydroxy-4-(4-(methylamino)phenyl)-3-buten-2-one (**20a**) was synthesized from 4'-(methylamino)acetophenone (104 mg, 697 μ mol) in 91% yield using the method described for the preparation of **13a**. 1H -NMR (400 MHz, CD_3OD) δ : 7.84 (d, $J = 8.0$ Hz, 2H), 6.57 (d, $J = 8.4$ Hz, 2H), 6.27 (s, 1H), 2.82 (s, 3H).

4-Hydrazinobenzoic acid (73 mg, 480 μ mol, 1.1 eq.) was dissolved in dry EtOH (5.0 mL), added 2 N HCl (250 μ L) and **20a** (104 mg, 424 μ mol). After stirring for 2.5 h at 75 $^\circ$ C, the reaction mixture was extracted two times with EtOAc, and washed with brine. The organic layer was dried over $MgSO_4$, filtered, and concentrated. The residue was purified by silica gel flash column chromatography ($CH_2Cl_2/MeOH = 10:1$) to afford **20b** (28 mg, 77.4 μ mol, 18%). 1H -NMR (500 MHz, CD_3OD) δ : 8.04 (d, $J = 8.5$ Hz, 2H), 7.43 (d, $J = 8.5$ Hz, 2H), 7.00 (d, $J = 8.5$ Hz, 2H), 6.77 (s, 1H), 6.54 (d, $J = 7.0$ Hz, 2H), 2.76 (s, 3H).

20c was synthesized from **20b** (28 mg, 77.5 μ mol) in 58% yield using the method described for the preparation of UTX-121. 1H -NMR (400 MHz, $CDCl_3$) δ : 8.03 (d, $J = 8.8$ Hz, 2H), 7.43 (d, $J = 9.2$ Hz, 2H), 7.01 (d, $J = 9.2$ Hz, 2H), 6.65 (s, 1H), 6.52 (d, $J = 8.8$ Hz, 2H), 3.92 (s, 3H), 2.85 (s, 3H); HRMS (ESI-TOF): m/z calcd. for $C_{19}H_{17}F_3N_3O_2$ $[M + H]^+$ 376.1273, found 376.1276.

Methyl 4-(5-(4-(dimethylamino)phenyl)-3-(trifluoromethyl)-1H-pyrazol-1-yl)benzoate (21c)

(*Z*)-4-(4-(dimethylamino)phenyl)-1,1,1-trifluoro-4-hydroxy-3-buten-2-one (**21a**) was synthesized from *p*-(dimethylamino)acetophenone (198 mg, 1.21 mmol) in 72% yield using the method described for the preparation of **13a**. 1H -NMR (400 MHz, $(CD_3)_2CO$) δ : 7.84 (d, $J = 8.8$ Hz, 2H), 6.66 (d, $J = 8.4$ Hz, 2H), 6.24 (s, 1H), 3.00 (s, 6H).

4-(5-(4-(Dimethylamino)phenyl)-3-(trifluoromethyl)-1H-pyrazol-1-yl)benzoic acid (**21b**) was synthesized from **21a** (202 mg, 779 μ mol) in 85% yield using the method described for the preparation of **13b**.

¹H-NMR (400 MHz, CD₃OD) δ: 8.06 (d, *J* = 8.4 Hz, 2H), 7.44 (d, *J* = 8.8 Hz, 2H), 7.08 (d, *J* = 9.2 Hz, 2H), 6.80 (s, 1H), 6.69 (d, *J* = 9.2 Hz, 2H), 2.96 (s, 6H).

21c was synthesized from **21b** (198 mg, 528 μmol) in 74% yield using the method described for the preparation of **13c**. ¹H-NMR (400 MHz, CDCl₃) δ: 8.03 (d, *J* = 8.8 Hz, 2H), 7.44 (d, *J* = 8.8 Hz, 2H), 7.05 (d, *J* = 9.2 Hz, 2H), 6.66 (s, 1H), 6.61 (d, *J* = 8.8 Hz, 2H), 3.93 (s, 3H), 2.98 (s, 6H); HRMS (ESI-TOF): *m/z* calcd. for C₂₀H₁₉F₃N₃O₂ [M + H]⁺ 390.1429, found 390.1430.

Methyl 4-(5-(cyclohex-1-en-1-yl)-3-(trifluoromethyl)-1*H*-pyrazol-1-yl)benzoate (22c)

(*Z*)-4-(cyclohex-1-en-1-yl)-1,1,1-trifluoro-4-hydroxy-3-buten-2-one (**22a**) was synthesized from 1-acetyl-1-cyclohexene (100 μL, 778 μmol) in 18% yield using the method described for the preparation of **9a**. ¹H-NMR (400 MHz, CD₃OD) δ: 6.79 (brs, 1H), 5.89 (brs, 1H), 2.27–2.19 (m, 4H), 1.69–1.58 (m, 4H).

4-(5-(Cyclohex-1-en-1-yl)-3-(trifluoromethyl)-1*H*-pyrazol-1-yl)benzoic acid (**22b**) was synthesized from **22a** (25 mg, 115 μmol) in 98% yield using the method described for the preparation of **2**. ¹H-NMR (400 MHz, CD₃OD) δ: 8.16 (d, *J* = 8.8 Hz, 2H), 7.63 (d, *J* = 8.8 Hz, 2H), 6.67 (s, 1H), 5.92–5.90 (m, 1H), 2.16–2.08 (m, 4H), 1.69–1.60 (m, 4H).

22c was synthesized from **22b** (37 mg, 110 μmol) in 70% yield using the method described for the preparation of **13c**. ¹H-NMR (400 MHz, CD₃OD) δ: 8.16 (d, *J* = 6.8 Hz, 2H), 7.65 (d, *J* = 6.8 Hz, 2H), 6.67 (s, 1H), 5.91–5.90 (m, 1H), 3.95 (s, 3H), 2.14–2.08 (m, 4H), 1.69–1.60 (m, 4H); HRMS (ESI-TOF): *m/z* calcd. for C₁₈H₁₈F₃N₂O₂ [M + H]⁺ 351.1320, found 351.1332.

Methyl 4-(5-cyclohexyl-3-(trifluoromethyl)-1*H*-pyrazol-1-yl)benzoate (23c)

(*Z*)-4-cyclohexyl-1,1,1-trifluoro-4-hydroxy-3-buten-2-one (**23a**) was synthesized from cyclohexyl methyl ketone (150 μL, 1.09 mmol) in 58% yield using the method described for the preparation of **13a**. ¹H-NMR (400 MHz, (CD₃)₂CO) δ: 5.52 (s, 1H), 2.15–2.09 (m, 1H), 1.73–1.71 (m, 4H), 1.41–1.19 (m, 6H).

4-(5-Cyclohexyl-3-(trifluoromethyl)-1*H*-pyrazol-1-yl)benzoic acid (**23b**) was synthesized from **23a** (98 mg, 441 μmol) in 97% yield using the method described for the preparation of **13b**. ¹H-NMR (400 MHz,

CD₃OD) δ : 8.22 (d, J = 8.8 Hz, 1H), 8.18 (d, J = 8.8 Hz, 1H), 7.60 (d, J = 8.8 Hz, 2H), 6.66 (s, 1H), 2.78–2.71 (m, 1H), 1.89–1.69 (m, 4H), 1.57–1.24 (m, 6H).

23c was synthesized from **23b** (96 mg, 284 μ mol) in 36% yield using the method described for the preparation of **13c**. ¹H-NMR (500 MHz, CDCl₃) δ : 8.19 (d, J = 9.0 Hz, 2H), 7.52 (d, J = 8.5 Hz, 2H), 6.48 (s, 1H), 3.97 (s, 3H), 2.70–2.64 (m, 1H), 1.86–1.70 (m, 4H), 1.42–1.20 (m, 6H); HRMS (ESI-TOF): m/z calcd. for C₁₈H₂₀F₃N₂O₂ [M + H]⁺ 353.1477, found 353.1475.

Methyl 4-(5-(pyridin-4-yl)-3-(trifluoromethyl)-1H-pyrazol-1-yl)benzoate (24c)

(*Z*)-1,1,1-trifluoro-4-hydroxy-4-(pyridin-4-yl)-3-buten-2-one (**24a**) was synthesized from 4-acetylpyridine (200 μ L, 1.82 mmol) in 71% yield using the method described for the preparation of **13a**. ¹H-NMR (400 MHz, (CD₃)₂CO) δ : 8.65 (d, J = 5.6 Hz, 2H), 7.76 (d, J = 5.6 Hz, 2H), 6.35 (s, 1H).

4-Hydrazinobenzoic acid (54 mg, 355 μ mol, 1.1 eq.) was dissolved in dry EtOH (4.5 mL), added 2 N HCl (190 μ L) and **24a** (73 mg, 336 μ mol). After stirring for 1.5 h at 75 °C, the reaction mixture was evaporated. The residue was dissolved in EtOAc and the precipitate was removed by filtration. The filtrate was evaporated to afford 4-(5-(pyridin-4-yl)-3-(trifluoromethyl)-1H-pyrazol-1-yl)benzoic acid (**24b**) (69 mg, 207 μ mol, 62%). ¹H-NMR (400 MHz, CD₃OD) δ : 8.55 (d, J = 6.4 Hz, 2H), 8.12 (d, J = 8.8 Hz, 2H), 7.48 (d, J = 8.8 Hz, 2H), 7.34 (d, J = 6.0 Hz, 2H), 7.21 (s, 1H).

24c was synthesized from **24b** (40 mg, 120 μ mol) in 55% yield using the method described for the preparation of **13c**. ¹H-NMR (400 MHz, CDCl₃) δ : 8.62 (d, J = 5.6 Hz, 2H), 8.09 (d, J = 8.8 Hz, 2H), 7.40 (d, J = 8.4 Hz, 2H), 7.13 (d, J = 6.0 Hz, 2H), 6.90 (s, 1H), 3.95 (s, 3H); HRMS (ESI-TOF): m/z calcd. for C₁₇H₁₃F₃N₃O₂ [M + H]⁺ 348.0960, found 348.0967.

Methyl 4-(5-(1-methyl-1H-pyrrol-3-yl)-3-(trifluoromethyl)-1H-pyrazol-1-yl)benzoate (25c)

(*Z*)-1,1,1-trifluoro-4-hydroxy-4-(1-methyl-1H-pyrrol-3-yl)-3-buten-2-one (**25a**) was synthesized from 3-acetyl-1-methyl pyrrole (300 μ L, 2.54 mmol) in 26% yield using the method described for the preparation of **13a**. ¹H-NMR (500 MHz, CD₃OD) δ : 7.31 (brs, 1H), 6.59 (s, 1H), 6.45 (s, 1H), 5.97 (brs, 1H),

3.66 (s, 3H).

4-(5-(1-Methyl-1*H*-pyrrol-3-yl)-3-(trifluoromethyl)-1*H*-pyrazol-1-yl)benzoic acid (**25b**) was synthesized from **25a** (49 mg, 224 μ mol) in 89% yield using the method described for the preparation of **13b**. ¹H-NMR (400 MHz, CD₃OD) δ : 8.13 (d, J = 8.8 Hz, 2H), 7.54 (d, J = 8.4 Hz, 2H), 6.73 (s, 1H), 6.65–6.61 (m, 2H), 5.85 (dd, J = 2.0, 2.8 Hz, 1H), 3.60 (s, 3H).

25c was synthesized from **25b** (45 mg, 134 μ mol) in 81% yield using the method described for the preparation of **13c**. ¹H-NMR (400 MHz, CDCl₃) δ : 8.09 (d, J = 8.8 Hz, 2H), 7.55 (d, J = 8.4 Hz, 2H), 6.60 (s, 1H), 6.53–6.47 (m, 2H), 5.89 (dd, J = 1.6, 2.8 Hz, 1H), 3.95 (s, 3H), 3.61 (s, 3H); HRMS (ESI-TOF): m/z calcd. for C₁₇H₁₅F₃N₃O₂ [M + H]⁺ 350.1116, found 350.1131.

Methyl 4-(5-(furan-2-yl)-3-(trifluoromethyl)-1*H*-pyrazol-1-yl)benzoate (**26c**)

(*Z*)-1,1,1-trifluoro-4-(furan-2-yl)-4-hydroxy-3-buten-2-one (**26a**) was synthesized from 2-acetylfuran (200 μ L, 1.99 mmol) in 51% yield using the method described for the preparation of **13a**. ¹H-NMR (400 MHz, (CD₃)₂CO) δ : 7.64 (d, J = 0.8 Hz, 1H), 7.10 (d, J = 2.8 Hz, 1H), 6.54–6.53 (m, 1H), 6.19 (s, 1H).

4-(5-(Furan-2-yl)-3-(trifluoromethyl)-1*H*-pyrazol-1-yl)benzoic acid (**26b**) was synthesized from **26a** (72 mg, 349 μ mol) in 84% yield using the method described for the preparation of **13b**. ¹H-NMR (400 MHz, CD₃OD) δ : 8.17 (d, J = 8.0 Hz, 2H), 7.57 (d, J = 2.0 Hz, 1H), 7.54 (d, J = 8.4 Hz, 2H), 7.05 (s, 1H), 6.49–6.48 (m, 1H), 6.31 (d, J = 3.6 Hz, 1H).

26c was synthesized from **26b** (41 mg, 127 μ mol) in 59% yield using the method described for the preparation of **13c**. ¹H-NMR (400 MHz, CDCl₃) δ : 8.15 (d, J = 8.8 Hz, 2H), 7.52 (d, J = 8.8 Hz, 2H), 7.43 (d, J = 1.6 Hz, 1H), 6.91 (s, 1H), 6.40–6.39 (m, 1H), 6.18 (d, J = 3.6 Hz, 1H), 3.96 (s, 3H); HRMS (ESI-TOF): m/z calcd. for C₁₆H₁₂F₃N₂O₃ [M + H]⁺ 337.0800, found 337.0779.

Methyl 4-(5-(thiophen-2-yl)-3-(trifluoromethyl)-1*H*-pyrazol-1-yl)benzoate (**27c**)

(*Z*)-1,1,1-trifluoro-4-hydroxy-4-(thiophen-2-yl)-3-buten-2-one (**27a**) was synthesized from 2-acetyltiophene (200 μ L, 1.85 mmol) in 91% yield using the method described for the preparation of **13a**. ¹H-

NMR (400 MHz, (CD₃)₂CO) δ : 7.55 (d, J = 3.6 Hz, 1H), 7.53 (d, J = 5.2 Hz, 1H), 7.06 (d, J = 4.4 Hz, 1H), 5.95 (s, 1H).

4-(5-(Thiophen-2-yl)-3-(trifluoromethyl)-1*H*-pyrazol-1-yl)benzoic acid (**27b**) was synthesized from **27a** (102 mg, 459 μ mol) in 93% yield using the method described for the preparation of **13b**. ¹H-NMR (400 MHz, CD₃OD) δ : 8.13 (d, J = 8.0 Hz, 2H), 7.54–7.52 (m, 3H), 7.06–7.04 (m, 2H), 7.01 (s, 1H).

27c was synthesized from **27b** (47 mg, 139 μ mol) in 59% yield using the method described for the preparation of **13c**. ¹H-NMR (400 MHz, CDCl₃) δ : 8.10 (d, J = 7.2 Hz, 2H), 7.49 (d, J = 8.8 Hz, 2H), 7.38 (d, J = 4.8 Hz, 1H), 6.99 (t, J = 4.0 Hz, 1H), 6.88 (d, J = 3.6 Hz, 1H), 6.82 (s, 1H), 3.95 (s, 3H); HRMS (ESI-TOF): m/z calcd. for C₁₆H₁₂F₃N₂O₂S [M + H]⁺ 353.0572, found 353.0571.

Methyl 4-(5-(naphthalen-2-yl)-3-(trifluoromethyl)-1*H*-pyrazol-1-yl)benzoate (28c)

60% NaH (237 mg, 5.93 mmol, 2.1 eq.) and 2'-acetonaphnone (490 mg, 2.88 mmol) were dissolved in dry THF (10 mL) under ice-cold. After stirring for 1 h under 0 °C, ethyl trifluoroacetate (515 μ L, 4.31 mmol, 1.5 eq.) was added, and the reaction mixture was stirred for 29 h at room temperature. The reaction mixture was acidified to pH 6 with 1 N HCl, extracted two times with EtOAc, and washed with brine. The organic layer was dried over MgSO₄, filtered, and concentrated. The residue was reprecipitated with EtOAc and n-hexane, purified by silica gel flash column chromatography (n-hexane/EtOAc = 2:1) to afford (*Z*)-1,1,1-trifluoro-4-hydroxy-4-(naphthalen-2-yl)-3-buten-2-one (**28a**) (286 mg, 1.07 mmol, 37%). ¹H-NMR (500 MHz, CD₃OD) δ : 8.54 (s, 1H), 8.07 (d, J = 8.5 Hz, 1H), 7.99–7.88 (m, 3H), 7.56–7.52 (m, 2H), 6.56 (s, 1H).

4-(5-(Naphthalen-2-yl)-3-(trifluoromethyl)-1*H*-pyrazol-1-yl)benzoic acid (**28b**) was synthesized from **28a** (51 mg, 192 μ mol) in 76% yield using the method described for the preparation of **2**. ¹H-NMR (400 MHz, (CD₃)₂CO) δ : 8.09 (d, J = 8.8 Hz, 2H), 8.03 (s, 1H), 7.95–7.89 (m, 3H), 7.60–7.55 (m, 4H), 7.37 (d, J = 6.8 Hz, 1H), 7.16 (s, 1H).

28c was synthesized from **28b** (38 mg, 99.4 μ mol) in 79% yield using the method described for the preparation of **13c**. ¹H-NMR (400 MHz, CDCl₃) δ : 8.01 (d, J = 6.8 Hz, 2H), 7.85–7.77 (m, 4H), 7.55–7.51 (m, 2H), 7.43 (d, J = 7.2 Hz, 2H), 7.19 (d, J = 8.8 Hz, 1H), 6.87 (s, 1H), 3.91 (s, 3H); HRMS (ESI-TOF): m/z calcd.

for C₂₂H₁₆F₃N₂O₂ [M + H]⁺ 397.1164, found 397.1163.

Methyl 4-(5-(2,3-dihydro-1*H*-inden-5-yl)-3-(trifluoromethyl)-1*H*-pyrazol-1-yl)benzoate (29c)

(*Z*)-4-(2,3-dihydro-1*H*-inden-5-yl)-1,1,1-trifluoro-4-hydroxy-3-buten-2-one (**29a**) was synthesized from 5-acetylidane (150 μ L, 999 μ mol) in 29% yield using the method described for the preparation of **13a**. ¹H-NMR (400 MHz, CD₃OD) δ : 7.78–7.72 (br, 2H), 7.23 (d, *J* = 7.2 Hz, 1H), 6.32 (brs, 1H), 2.94–2.91 (m, 4H), 2.13–2.06 (m, 2H).

4-(5-(2,3-Dihydro-1*H*-inden-5-yl)-3-(trifluoromethyl)-1*H*-pyrazol-1-yl)benzoic acid (**29b**) was synthesized from **29a** (50 mg, 195 μ mol) in 96% yield using the method described for the preparation of **13b**. ¹H-NMR (400 MHz, CD₃OD) δ : 8.04 (d, *J* = 9.2 Hz, 2H), 7.42 (d, *J* = 8.8 Hz, 2H), 7.20 (d, *J* = 8.0 Hz, 1H), 7.15 (s, 1H), 6.99 (d, *J* = 8.0 Hz, 1H), 6.88 (s, 1H), 2.93–2.84 (m, 4H), 2.11–2.04 (m, 2H).

29c was synthesized from **29b** (44 mg, 118 μ mol) in 42% yield using the method described for the preparation of **13c**. ¹H-NMR (500 MHz, CDCl₃) δ : 8.03 (d, *J* = 8.5 Hz, 2H), 7.41 (d, *J* = 8.5 Hz, 2H), 7.16 (d, *J* = 7.5 Hz, 1H), 7.11 (s, 1H), 6.93 (d, *J* = 7.5 Hz, 1H), 6.72 (s, 1H), 3.92 (s, 3H), 2.93–2.85 (m, 4H), 2.12–2.06 (m, 2H); HRMS (ESI-TOF): *m/z* calcd. for C₂₁H₁₈F₃N₂O₂ [M + H]⁺ 387.1320, found 387.1334.

Methyl 4-(5-(benzo[*d*][1,3]dioxol-5-yl)-3-(trifluoromethyl)-1*H*-pyrazol-1-yl)benzoate (30c)

(*Z*)-4-(benzo[*d*][1,3]dioxol-5-yl)-1,1,1-trifluoro-4-hydroxy-3-buten-2-one (**30a**) was synthesized from 3',4'-(methylenedioxy)acetophenone (199 mg, 1.21 mmol) in 80% yield using the method described for the preparation of **13a**. ¹H-NMR (400 MHz, (CD₃)₂CO) δ : 7.55–7.35 (m, 2H), 6.83 (d, *J* = 8.4 Hz, 2H), 6.22 (s, 1H), 6.02 (s, 2H).

4-(5-(Benzo[*d*][1,3]dioxol-5-yl)-3-(trifluoromethyl)-1*H*-pyrazol-1-yl)benzoic acid (**30b**) was synthesized from **30a** (103 mg, 396 μ mol) in 91% yield using the method described for the preparation of **13b**. ¹H-NMR (400 MHz, CD₃OD) δ : 8.07 (d, *J* = 8.0 Hz, 2H), 7.44 (d, *J* = 8.4 Hz, 2H), 6.88 (s, 1H), 6.84–6.77 (m, 2H), 6.74 (s, 1H), 5.99 (s, 2H).

30c was synthesized from **30b** (101 mg, 268 μ mol) in 82% yield using the method described for the

preparation of **13c**. ¹H-NMR (400 MHz, CDCl₃) δ: 8.05 (d, *J* = 8.4 Hz, 2H), 7.41 (d, *J* = 8.8 Hz, 2H), 6.79–6.64 (m, 4H), 6.00 (s, 2H), 3.93 (s, 3H); HRMS (ESI-TOF): *m/z* calcd. for C₁₉H₁₄F₃N₂O₄ [M + H]⁺ 391.0906, found 391.0894.

3.2. Cell culture

HT-1080 human sarcoma cells were obtained from the American Type Culture Collection (Manassas, VA, USA) and were maintained in Dulbecco's modified Eagle's medium (DMEM; Sigma-Aldrich, St. Louis, Mo USA, or Wako Pure Chemical, Osaka, Japan). The culture medium was supplemented with 10% fetal bovine serum (FBS), and the cells were cultured in a humidified atmosphere of 5% CO₂ at 37 °C.

3.3. *In vitro* WST-8 assay

In vitro cytotoxicity was examined using a colorimetric assay with the Cell Counting Kit-8 (Dojindo Laboratories, Kumamoto, Japan), according to the manufacturer's instructions. Briefly, HT-1080 cells were seeded at a density of 4 × 10³ cells/well in a 96-well plate and cultured for 24 h. Serial dilutions of each compound, dissolved in dimethyl sulfoxide (DMSO), were added to the culture medium at concentrations of 3.125–100 μM. After 48 h of incubation, the medium was replaced with fresh medium containing the WST-8 reagent. After 1 h, the absorbance in each well was measured at 460 nm using a microplate spectrophotometer, ImmunoMini NJ-2300 (BioTec, Tokyo, Japan).

The percentage of cell growth inhibition was calculated by applying the following formula: percentage of cell growth inhibition = (1-[T/C]) × 100, where C and T are the mean absorbance values of the control and treated groups, respectively. The IC₅₀ value was measured graphically from the dose-response curve with at least three drug concentration points.

3.4. Gelatin zymography

HT-1080 cells (1 × 10⁵ cells/well) were seeded in a 6-well tissue culture plate and cultured in 10% FBS/DMEM overnight. After washing twice with phosphate-buffered saline (PBS), the cells were serum-starved

with 0.5% FBS/DMEM for 6 h (or overnight), and then treated with the inhibitors for 24 h. The conditioned medium (CM) was analyzed by gelatin zymography. MMP-2 and MMP-9 levels in CM were measured by adding an equal volume of sample buffer. The samples were separated by electrophoresis on an SDS-polyacrylamide gel containing gelatin (Difco, Sparks, MD, USA) labeled with Alexa Fluor 680 (Molecular Probes, Eugene, OR, USA). The gels were processed and monitored using an Odyssey infrared imaging system (LI-COR, Lincoln, NE, USA) against the normalized density of the target band in the control sample.

3.5. Immunofluorescence staining

HT-1080 cells were transfected with FLAG epitope-tagged MT1-MMP plasmid, serum starved, and treated with the inhibitors for 24 h. For cell surface staining, the cells were incubated for 30 min at 37 °C with an anti-FLAG antibody (Sigma-Aldrich). After washing, the cells were fixed with 4% paraformaldehyde for 15 min. Alternatively, the cells were fixed and permeabilized with 0.5% Triton X-100 and reacted with an anti-FLAG antibody. The cells were visualized with Alexa™488-conjugated goat anti-mouse antibody, Hoechst 33342, and rhodamine-labeled phalloidin (Molecular Probes).

3.6. COX-2 inhibition assay

COX-2 inhibitory activity was assessed using the COX-2 (human) Inhibitor Screening Assay Kit (Cayman Chemical, Ann Arbor, MI, USA) according to the manufacturer's instructions. In brief, COX-2 was inactivated by placing it in boiling water for 3 min. Compounds dissolved in DMSO were added to each test tube, and 10 µL of DMSO was added to the control and background tubes. All tubes were incubated for 10 min at 37 °C in a heat block. Arachidonic acid (10 µL) was added to the reaction tubes to initiate the reaction. The tubes were quickly mixed and incubated for 2 min at 37 °C. Saturated stannous chloride solution (30 µL) was added to each reaction tube to stop enzyme catalysis. All tubes were removed from the heat block, vortexed, and incubated for 5 min at room temperature. The amount of prostaglandin in the tubes was evaluated by ELISA.

3.7. Wound healing assay

Serum-starved HT-1080 cells were treated with the inhibitors in Opti-MEM for 24 h and allowed to adhere to fibronectin-coated dishes for 2 h at 37 °C. Subsequently, confluent cell monolayers were scraped off. After adding Opti-MEM containing inhibitors, wound closure was monitored for 15 h.

3.8. Cell invasion assay

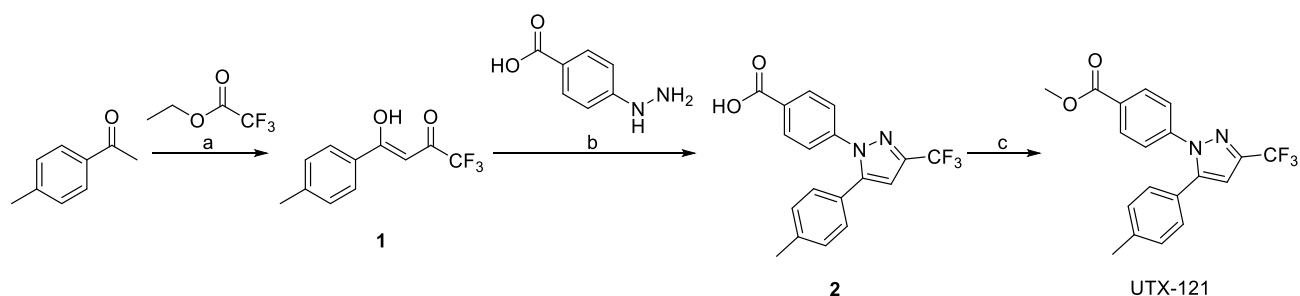
Cell invasion was assayed using a modified Boyden chamber consisting of Transwell membrane filters (Corning Costar, Cambridge, MA, USA). The upper surfaces of the membranes were coated with 1 mg/ml Matrigel matrix (BD Biosciences, Lexington, KY, USA) and placed in 24-well tissue culture plates filled with 600 ml Opti-MEM with inhibitors. Serum-starved HT-1080 cells (2×10^5 cells) were suspended in 100 mL Opti-MEM, added to each Transwell chamber, and cultured for 6 h as pretreatment. Subsequently, fibronectin (Asahi Techno Glass, Tokyo, Japan) was added to the lower chambers (final concentration: 10 mg/mL). After further cultivation for 16 h, the membranes were fixed and stained. The number of crystal violet-stained cells on the lower surface was counted under a microscope.

4 Results

4.1. Design and synthesis of UTX-121

To develop a novel antimetastatic agent, we first focused on the sulfonamide moiety of celecoxib and designed a new derivative based on the bioisosterism principle. The carboxylic acid is known to be a bioisostere of the sulfonamide, but it has poor cell permeability due to its extremely high polarity. Therefore, we designed UTX-121 with enhanced liposolubility by protecting the carboxylic acid with a methyl ester.

UTX-121 was prepared as shown in Scheme 1. Compound **1** was synthesized by the Claisen condensation reaction with 4'-methylacetophenone and ethyl trifluoroacetate in THF. Subsequently, compound **1** and 4-hydrazinobenzoic acid were cyclized in EtOH to afford compound **2**. Finally, the target compound was successfully synthesized by the esterification of compound **2** using SOCl₂.



Scheme 1. (a) NaH, THF, r.t., 3.5 h; (b) 2N HCl, EtOH, 75 °C, 0.5 h; (c) SOCl₂, MeOH, r.t., 19.5 h. (Yamahana H. *et al.*, *Biochem. Biophys. Res. Commun.*, **2020**, 521(1), 137–144.)

4.2. MMP inhibitory activity of UTX-121

MMP-2/9 inhibitory activities of UTX-121 were evaluated by gelatin zymography. In this study, HT-1080 cells, which express little COX-2, were used to evaluate COX-2-independent MMPs inhibitory activities. The results showed that the MMPs inhibitory activity of celecoxib was very limited. In contrast, UTX-121 significantly inhibited MMP-9 production and MMP-2 activation. Moreover, these inhibitory activities were dose-dependent. (Fig. 6)

We then examined the MT1-MMP inhibitory activity of UTX-121 via immunofluorescence staining. It was revealed that the expression level of MT1-MMP on the cell surface was sharply decreased by the

application of UTX-121. In contrast, there was no significant change to the expression level of MT1-MMP in permeabilized cells. (Fig. 7)

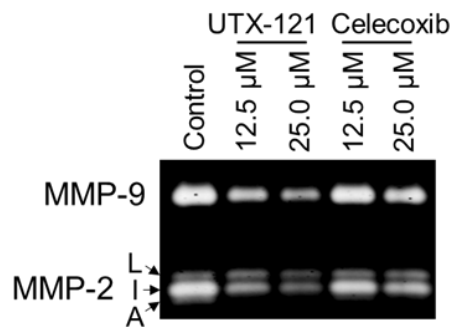


Fig. 6. MMP-2/9 inhibitory activity of UTX-121. HT-1080 cells were treated with UTX-121 or celecoxib for 24 h, and the CM was examined by gelatin zymography. L, latent form; I, intermediate form; A, active form of MMP-2. (Yamahana H. *et al.*, *Biochem. Biophys. Res. Commun.*, **2020**, 521(1), 137–144.)

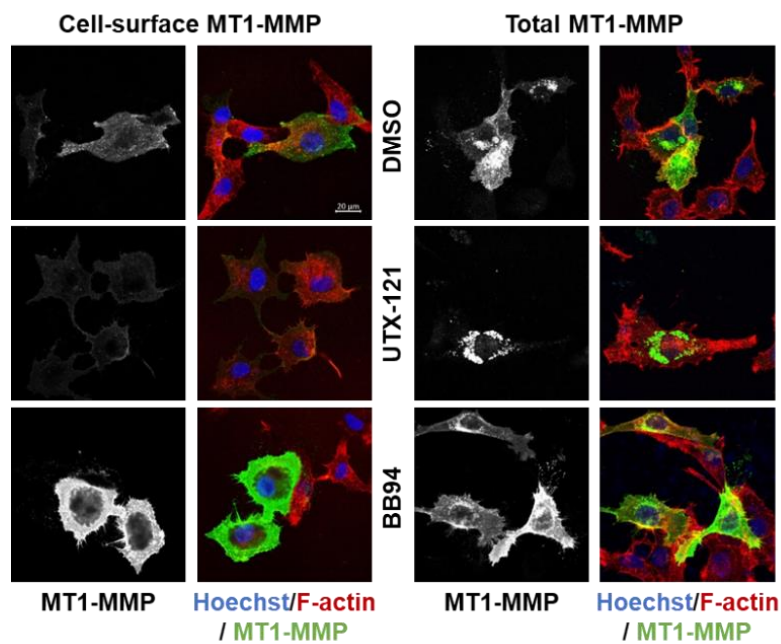


Fig. 7. MT1-MMP inhibitory activity of UTX-121. HT-1080 cells were treated with UTX-121 (25 μM) or BB94 (2 μM) for 12 h, and the localization of MT1-MMP was evaluated by immunofluorescence staining. Cell-surface indicates non-permeabilized cells; Total indicates permeabilized cells. (Yamahana H. *et al.*, *Biochem. Biophys. Res. Commun.*, **2020**, 521(1), 137–144.)

4.3. The effect of UTX-121 on cell invasion

We investigated the effect of UTX-121 on the cell migration potency by wound healing assay, and found that UTX-121 inhibited the migration of HT-1080 cells (Fig. 8A). We also evaluated the invasion inhibitory activity of UTX-121. The results showed that the number of invasive cells decreased to 57.9% for cells treated with celecoxib and to 29.9% for cells treated with UTX-121, indicating that UTX-121 has a potent inhibitory effect on the invasive capacity (Fig. 8B).

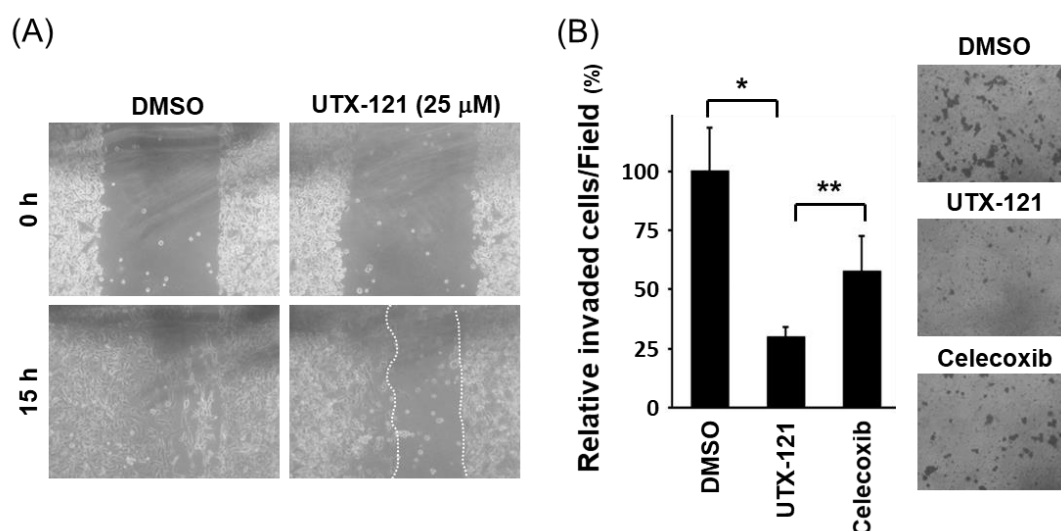
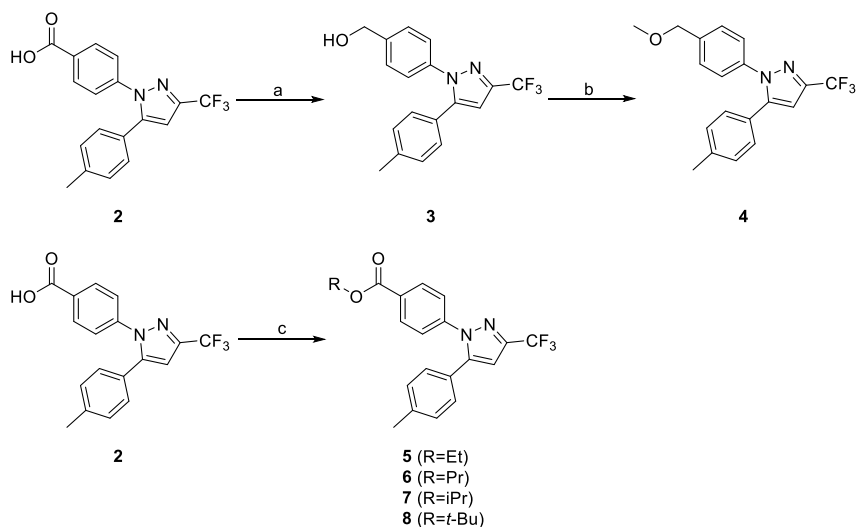


Fig. 8. The effect of UTX-121 on cell invasion. (A) Wound healing assay for HT-1080 cells. White dotted lines indicate unclosed wound area; (B) Cell invasion assay for HT-1080 cells. * $P < 0.01$, ** $P < 0.05$. (Yamahana H. *et al.*, *Biochem. Biophys. Res. Commun.*, **2020**, 521(1), 137–144.)

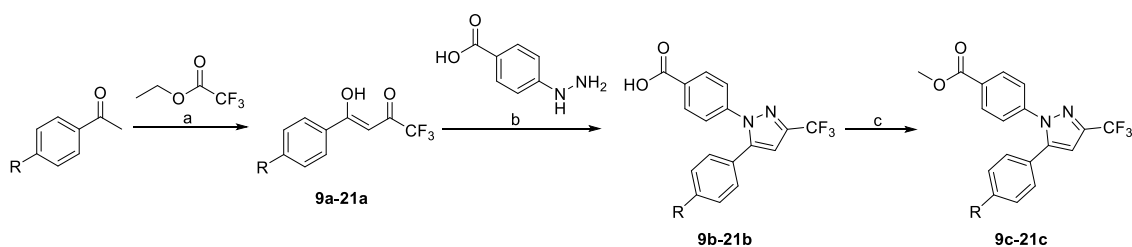
4.4. Design and synthesis of UTX-121 derivatives

In order to enhance the MMP-2/9 inhibitory activities of UTX-121 more, we designed various UTX-121 derivatives. First, to investigate the importance of the methyl ester, we designed derivatives in which the methyl ester was substituted with an alcohol (compound **3**) or an ether (compound **4**). We also examined the alkyl chain length of methyl ester (compounds **5–8**). We then focused on the *p*-tolyl group of UTX-121. We designed compounds with various functional groups introduced into the methyl group of the *p*-tolyl moiety (compounds **9c–21c**) and compounds with various aromatics substituted for the *p*-tolyl moiety (compounds **22c–30c**), and evaluated their antitumor and MMP-2/9 inhibitory activities.

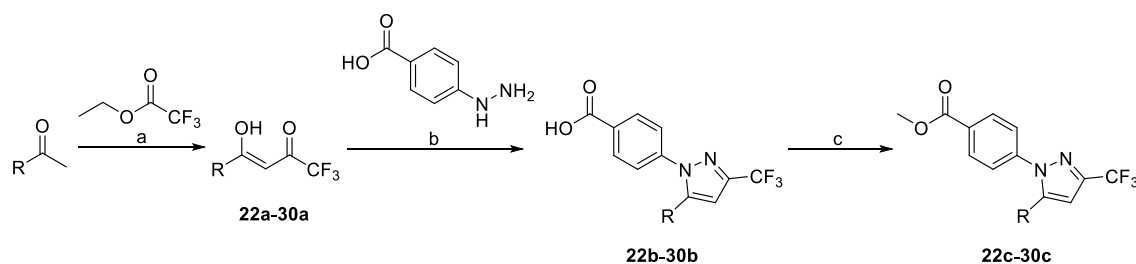
UTX-121 derivatives were synthesized as shown in Schemes 2–4. Compound **2** was reduced by LiAlH_4 to give compound **3**, and followed by etherification to give compound **4**. Compounds **5–8** were synthesized by the esterification of compound **2**. We successfully prepared compounds **9c–30c** by applying the same method as UTX-121.



Scheme 2. (a) LiAlH_4 , THF, r.t., 1.5 h; (b) CH_3I , NaH, THF, r.t., 19 h; (c) **5–7**: SOCl_2 , EtOH (or 1-propanol or 2-propanol), r.t., 18–24 h; **8**: benzyltriethylammonium chloride, K_2CO_3 , 2-bromo-2-methylpropane, *N,N*-dimethylacetamide, 55 °C, 19 h. (Reproduced in part with permission from *Chem. Pharm. Bull.*, Vol. 69, No. 10, Pages 1017–1028, Copyright [2021] The Pharmaceutical Society of Japan.)



Scheme 3. (a) NaH, THF (or *tert*-butyl methyl ether), r.t., 0.5–22 h; (b) 2 N HCl, EtOH, 75 °C, 0.5–3 h; (c) SOCl_2 , MeOH, r.t., 17.5–24 h. (Reproduced in part with permission from *Chem. Pharm. Bull.*, Vol. 69, No. 10, Pages 1017–1028, Copyright [2021] The Pharmaceutical Society of Japan.)



Scheme 4. (a) NaH, THF (or *tert*-butyl methyl ether), r.t., 1–26 h; (b) 2 N HCl, EtOH, 75 °C, 0.5–1.5 h; (c) SOCl₂, MeOH, r.t., 18–23.5 h. (Reproduced in part with permission from *Chem. Pharm. Bull.*, Vol. 69, No. 10, Pages 1017–1028, Copyright [2021] The Pharmaceutical Society of Japan.)

4.5. Antitumor activity of UTX-121 derivatives

We assessed the antitumor activities of UTX-121 derivatives by WST-8 assay. The IC₅₀ values for each compound are shown in Tables 1–3. The antitumor activity of compound **4** was at the similar level as UTX-121, while compound **3** showed stronger antitumor activity than UTX-121. Compounds **5–8** exhibited no antitumor activities. (Table 1)

The introduction of halogens (F, Cl, Br) or NHMe into UTX-121 (compounds **9c–11c**, **20c**) significantly enhanced the antitumor activity. It was demonstrated that compound **12c** (H) possessed the antitumor activity comparable to UTX-121. Among them, compound **17c** (OH) showed the most potent antitumor activity of all the UTX-121 derivatives. (Table 2)

Regarding compounds in which the *p*-tolyl group of UTX-121 was substituted with other aromatic groups, modest antitumor activity was observed in compounds **22c**, **23c**, **25c–27c**. On the other hand, compounds **24c**, **28c–30c** had no significant antitumor activities. (Table 3)

4.6. MMP-2/9 inhibitory activity of UTX-121 derivatives

The MMP-2/9 inhibitory activities of UTX-121 derivatives were evaluated by gelatin zymography. Tables 1–3 present the relative band densities of each derivative. Compound **4** had comparable MMP-2/9 inhibitory activities to those of UTX-121, while the substitution of the methyl ester with alcohol (compound **3**) attenuated these activities. There were no significantly higher MMPs inhibitory activities for compounds **5–7**

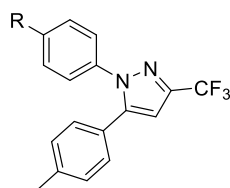
than UTX-121, and compound **8** suppressed MMP-2 expression and pro MMP-2 activation to the same extent as UTX-121. (Table 1)

When halogens were introduced into the methyl group (compounds **9c–11c**), the MMP-2/9 inhibitory activities were markedly enhanced, especially compounds **9c** and **10c**, which showed the highest activities among all UTX-121 derivatives. The suppressive effects of compounds **12c** and **15c** on MMP-2/9 production and pro MMP-2 activation were equivalent to those of UTX-121. In addition, compounds **17c** and **20c** exerted potent inhibitory activity on MMP-9 production. (Table 2)

Table 3 summarizes the MMPs inhibitory activities of compounds **22c–30c**. Compounds **22c** and **23c** suppressed MMP-2 expression and activation at the same level as UTX-121, and showed slightly higher inhibitory activity than UTX-121 only for MMP-9. However, for compounds **24c–30c**, there were no marked MMPs inhibitory activities. (Table 3)

4.7. COX-2 inhibitory activity of UTX-121 derivatives

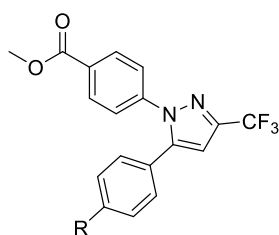
We determined the COX-2 inhibition rate of each derivative at 200 μM using the COX-2 (human) Inhibitor Screening Assay Kit. No compounds showed high COX-2 inhibitory activity, and even compound **25c** with the highest inhibition rate had the IC_{50} value of 10.1 μM . Taking into account that the IC_{50} value of celecoxib for COX-2 is 0.020 μM (reported IC_{50} value: 0.040 μM [20]), it is revealed that derivatives designed in this work exhibited much less COX-2 inhibitory activity than celecoxib.

Table 1Structure-activity relationship of compounds **3–8**.

Compound	R	IC ₅₀ (μM) ^a	Relative amount			ClogP ^e	COX-2 inhibition rate (%) ^f
			total MMP-9 ^b	total MMP-2 ^c	active MMP-2 ^d		
BB94	-	-	1.09	0.585	0.102	-	-
UTX-121		87.7	0.690	0.629	0.637	5.86	IC ₅₀ : 237 μM
3		38.3	0.863	0.942	1.39	4.80	61.9
4		77.9	0.710	0.549	0.528	5.64	N.D.
5		>100	0.837	0.649	0.665	6.38	1.73
6		>100	0.855	0.667	0.690	6.91	N.D.
7		>100	0.760	0.642	0.696	6.69	N.D.
8		>100	0.889	0.615	0.566	7.09	N.D.

^a Antitumor activity in HT-1080 cells; ^b Band density of total MMP-9;^c Band density of total MMP-2 (latent + active MMP-2); ^d Band density of active MMP-2;^e Calculated using ChemDraw 19.1; ^f COX-2 inhibition rate at 200 μM.

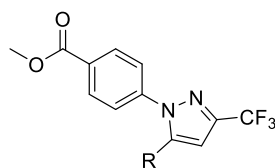
(Reproduced in part with permission from *Chem. Pharm. Bull.*, Vol. 69, No. 10, Pages 1017–1028, Copyright [2021] The Pharmaceutical Society of Japan.)

Table 2Structure-activity relationship of compounds **9c–21c**.

Compound	R	IC ₅₀ (μ M) ^a	Relative amount			ClogP ^e	COX-2 inhibition rate (%) ^f
			total MMP-9 ^b	total MMP-2 ^c	active MMP-2 ^d		
BB94	-	-	1.09	0.585	0.102	-	-
UTX-121	Me	87.7	0.690	0.629	0.637	5.86	IC ₅₀ : 237 μ M
9c	F	38.1	0.300	0.338	0.470	5.50	N.D.
10c	Cl	33.2	0.239	0.248	0.325	6.07	34.0
11c	Br	36.0	0.353	0.454	0.522	6.22	19.3
12c	H	76.6	0.533	0.718	0.847	5.36	43.9
13c	Et	>100	0.742	0.743	0.706	6.38	8.90
14c	CF ₃	>100	0.892	0.843	0.811	6.24	40.5
15c	CN	>100	0.561	0.612	0.547	4.79	78.5
16c	SMe	>100	0.825	0.929	0.964	5.92	44.0
17c	OH	18.0	0.137	0.599	0.787	4.73	32.6
18c	OMe	>100	0.756	0.796	0.872	5.30	23.1
19c	NO ₂	>100	0.911	0.941	0.957	5.10	67.6
20c	NHMe	34.5	0.472	0.645	0.823	4.90	47.6
21c	NMe ₂	>100	0.807	0.913	0.888	5.55	23.7

^a Antitumor activity in HT-1080 cells; ^b Band density of total MMP-9;^c Band density of total MMP-2 (latent + active MMP-2); ^d Band density of active MMP-2;^e Calculated using ChemDraw 19.1; ^f COX-2 inhibition rate at 200 μ M.(Reproduced in part with permission from *Chem. Pharm. Bull.*, Vol. 69, No. 10, Pages 1017–1028, Copyright

[2021] The Pharmaceutical Society of Japan.)

Table 3Structure-activity relationship of compounds **22c–30c**.

Compound	R	IC ₅₀ (μM) ^a	Relative amount			ClogP ^e	COX-2 inhibition rate (%) ^f
			total MMP-9 ^b	total MMP-2 ^c	active MMP-2 ^d		
BB94	-	-	1.09	0.585	0.102	-	-
UTX-121		87.7	0.690	0.629	0.637	5.86	IC ₅₀ : 237 μM
22c		61.0	0.595	0.787	0.874	5.57	N.D.
23c		71.2	0.584	0.697	0.716	5.65	N.D.
24c		>100	0.759	1.04	1.12	3.87	57.5
25c		78.0	0.832	0.910	0.999	4.44	95.9 IC ₅₀ : 10.1 μM
26c		81.2	0.944	0.976	1.04	4.74	N.D.
27c		68.6	0.733	0.957	1.15	5.22	25.1
28c		>100	0.953	1.05	1.19	6.53	9.57
29c		>100	0.807	0.700	0.710	6.37	58.4
30c		>100	0.772	0.731	0.897	5.33	26.5

^a Antitumor activity in HT-1080 cells; ^b Band density of total MMP-9;^c Band density of total MMP-2 (latent + active MMP-2); ^d Band density of active MMP-2;^e Calculated using ChemDraw 19.1; ^f COX-2 inhibition rate at 200 μM.

(Reproduced in part with permission from *Chem. Pharm. Bull.*, Vol. 69, No. 10, Pages 1017–1028, Copyright [2021] The Pharmaceutical Society of Japan.)

5 Discussion

In this study, we found that UTX-121, in which the sulfonamide group of celecoxib was modified to a methyl ester, had better MMP-2/9 inhibitory activities than celecoxib. Additionally, it was shown that the expression level of MT1-MMP on the cell surface was drastically reduced in UTX-121-treated cells, while the expression level of MT1-MMP on the whole-cell remained unchanged. MT1-MMP is expressed on the cell surface in its activated form, which leads to the activation of MMP-2 and MMP-9. Therefore, it is suggested that UTX-121 inhibits the activation of MMP-2 and also the expression of MMP-9 by inhibiting the cell surface expression of MT1-MMP, which leads to the inhibition of migration and invasion of cancer cells. Furthermore, UTX-121 exhibited little COX-2 inhibitory activity. Thus, it is indicated that the antitumor and MMP inhibitory activities of UTX-121 are mediated by a COX-2-independent pathway.

We then designed various UTX-121 derivatives to enhance the MMP-2/9 inhibitory activities of UTX-121 further. At first, the effects of methyl esters on antitumor and MMPs inhibitory activities were investigated. For compound **3**, only the antitumor activity was higher than that of UTX-121, but the MMP-2/9 inhibitory activities were not sufficient. The potency of compound **4** in suppressing tumor proliferation, MMP-2/9 expression, and pro MMP-2 activation was equivalent to that of UTX-121, and no remarkable improvement in efficacy was observed. The extension of the alkyl chain of the methyl ester (compounds **5–8**) led to less antitumor or MMP-2/9 inhibitory activities. Based on these results, we concluded that the methyl ester (C1) was the most suitable for exerting both antitumor and MMPs inhibitory activities.

In the next, we focused on the *p*-tolyl group of UTX-121, especially the methyl moiety. The introduction of halogens (compounds **9c–11c**) markedly improved the antitumor, MMP-2/9 expression, and pro MMP-2 activation inhibitory activities. The ClogP of compounds **9c–11c** was approximately 6, which is equivalent to that of UTX-121, suggesting that a certain extent of hydrophobicity must be secured in order to exert these activities. One of the reasons for the slight decrease in activities of compound **11c** might be attributed to the atomic size of Br; Cl and Br have a similar size as methyl and isopropyl groups, respectively. This is probably because the binding pocket of the target molecule is limited in size and Br did not well interact with the pocket due to its larger size. Compounds **17c** and **20c** also had significant antitumor activity, but the MMPs

inhibitory activities were only exhibited for MMP-9, not MMP-2. One thing these two derivatives have in common is that their ClogP values were much lower than those of the other derivatives. This implies that they had high polarity, indicating that their uptake into the cells was not efficient, or that their binding to the target hydrophobic pocket was not enough. Therefore, it is speculated that there might be a different mechanism of action for compounds **17c** and **20c** from that of UTX-121. Compound **15c** had moderate MMP-2/9 inhibitory activities, though it did not exert the antitumor activity. The cyano group is well known as the bioisostere of halogens. The results of compounds **9c–11c** suggested that the molecular size was also an essential factor for various activities, thus it is assumed that the efficacy of compound **15c** was lower than that of halogen-substituted compounds. Additionally, there was no correlation between the σ value, which describes the electronic effect of the substituent on the benzene ring, and the antitumor/MMPs inhibitory activities, indicating that the electronic effect was not significant.

Considering that the electronic effect did not affect the various activities, we also designed new derivatives in which the *p*-tolyl moiety was converted into various aromatic rings. Compounds with cyclohexene (compound **22c**) or cyclohexane (compound **23c**) had the highest MMP-2/9 expression and pro MMP-2 activation inhibitory activities among compounds **22c–30c**. These two derivatives have ClogP values of around 6, as do the halogen-substituted ones. This result also supports the hypothesis that some extent of hydrophobicity is essential to achieve both antitumor and MMPs inhibitory activities. Compounds in which the *p*-tolyl group was substituted with heterocycles (compounds **24c–27c**) showed stronger suppressive effects on MMP-9 as compared to MMP-2. Since these compounds have lower ClogP values, it is considered that their mechanisms of action might differ from that of UTX-121 as well as compounds **17c** and **20c**. Compounds **28c–30c** were not efficacious despite possessing some level of hydrophobicity. This was probably because the molecular size was too large to access the binding site of the target. Furthermore, COX-2 inhibitory activity was found to be extremely low for all UTX-121 derivatives. There was also no correlation between COX-2 inhibitory activity and antitumor/MMP-2/9 inhibitory activities. Therefore, the antitumor, MMP-2/9 expression, and pro MMP-2 activation inhibitory activities are considered to be mediated by a COX-2-independent pathway.

Finally, among the compounds which showed the antitumor activity, a weak correlation between the

antitumor activity and MMPs inhibitory activities was revealed ($r = 0.68$ (vs total MMP-9), 0.38 (vs total MMP-2), 0.32 (vs active MMP-2)). Cancer cells degrade the ECM through the effects of MMPs to secure their own proliferation space (Tumor jailbreak) [30]. Therefore, it is considered that UTX-121 derivatives act on the common targets involved in the cell proliferation and MMPs expression/activation, thereby disturbing the formation of the proliferation space and consequently exerting antitumor effects.

6 Conclusion

We successfully developed UTX-121 by substituting the sulfonamide group of celecoxib with a methyl ester. UTX-121 inhibited MT1-MMP-mediated MMP-2 activation and MMP-9 production, and also suppressed the migration and invasion of cancer cells. Then, in order to improve MMP-2/9 inhibitory activities of UTX-121 more, we designed and synthesized various UTX-121 derivatives by the structure-activity relationship approach. Among them, compounds **9c** and **10c**, in which F or Cl was introduced into UTX-121, exhibited more potent antitumor activity than UTX-121 and strongly suppressed MMP-2/9 expression and pro MMP-2 activation. These results suggest that compounds **9c** and **10c** could be potential lead compounds for the development of anticancer and antimetastatic agents targeting MMPs.

Acknowledgement

This thesis is a summary of my studies at the graduate school of Tokushima University. I would like to express my sincere gratitude to Professor Uto of Tokushima University for his extensive supervision as my academic advisor. Dr. Yamada, Associate Professor in the same department, provided me with many detailed pieces of advice. I would like to express my deep appreciation here. I would also like to show special thanks to Associate Professor Endo and Professor Takino of Kanazawa University for their generous contribution to the execution of this research. Several research resources were kindly supported by Extramural Collaborative Research Grant of Cancer Research Institute, Kanazawa University. In addition, this doctoral degree thesis was

examined by Professor Nakamura, Professor Matsuki, and Associate Professor Asada of Tokushima University. Finally, this thesis referenced figures, schemes, and tables from the following two articles; Yamahana H. *et al.*, *Biochem. Biophys. Res. Commun.*, **2020**, 521(1), 137–144 and Yamahana H. *et al.*, *Chem. Pharm. Bull.*, **2021**, 69(10), 1017–1028. I would like to take this opportunity to express my heartfelt thanks to all those who contributed to this study.

References

- [1] Kalluri R., Weinberg R. A., The basics of epithelial-mesenchymal transition. *J. Clin. Invest.*, **2009**, 119(6), 1420–1428.
- [2] Huber M. A., Kraut N., Beug H., Molecular requirements for epithelial-mesenchymal transition during tumor progression. *Curr. Opin. Cell Biol.*, **2005**, 17(5), 548–558.
- [3] Lambert A. W., Pattabiraman D. R., Weinberg R. A., Emerging biological principles of metastasis. *Cell*, **2017**, 168(4), 670–691.
- [4] Liu A., Wei L., Gardner W. A., Deng C. X., Man Y. G., Correlated alterations in prostate basal cell layer and basement membrane. *Int. J. Biol. Sci.*, **2009**, 5(3), 276–285.
- [5] Mylonas C. C., Lazaris A. C., Colorectal cancer and basement membranes: clinicopathological correlations. *Gastroenterol. Res. Pract.*, **2014**, 2014, 580159.
- [6] Frantz C., Stewart K. M., Weaver V. M., The extracellular matrix at a glance. *J. Cell Sci.*, **2010**, 123(4), 4195–4200.
- [7] Lu P., Weaver V. M., Werb Z., The extracellular matrix: a dynamic niche in cancer progression. *J. Cell Biol.*, **2012**, 196(4), 395–406.
- [8] Walker C., Mojares E., Del Río Hernández A., Role of extracellular matrix in development and cancer progression. *Int. J. Mol. Sci.*, **2018**, 19(10), 3028.
- [9] Kalluri R., Basement membranes: structure, assembly and role in tumour angiogenesis. *Nat. Rev. Cancer*, **2003**, 3, 422–433.

- [10] Egeblad M., Rasch M.G., Weaver V.M., Dynamic interplay between the collagen scaffold and tumor evolution. *Curr. Opin. Cell Biol.*, **2010**, 22(5), 697–706.
- [11] Gatseva A, Sin Y. Y., Brezzo G., Van Agtmael T., Basement membrane collagens and disease mechanisms. *Essays Biochem.*, **2019**, 63(3), 297–312.
- [12] Page-McCaw A., Ewald A. J., Werb Z., Matrix metalloproteinases and the regulation of tissue remodelling. *Nat. Rev. Mol. Cell Biol.*, **2007**, 8(3), 221–233.
- [13] Kessenbrock K., Plaks V., Werb Z., Matrix metalloproteinases: regulators of the tumor microenvironment. *Cell*, **2010**, 141(1), 52–67.
- [14] Egeblad M., Werb Z., New functions for the matrix metalloproteinases in cancer progression. *Nat. Rev. Cancer*, **2002**, 2, 161–174.
- [15] Roh M. R., Zheng Z., Kim H. S., Kwon J. E., Jeung H. C., Rha S. Y., Chung K. Y., Differential expression patterns of MMPs and their role in the invasion of epithelial premalignant tumors and invasive cutaneous squamous cell carcinoma. *Exp. Mol. Pathol.*, **2012**, 92(2), 236–242.
- [16] Sheen-Chen S. M., Chen H. S., Eng H. L., Sheen C. C., Chen W. J., Serum levels of matrix metalloproteinase 2 in patients with breast cancer. *Cancer Lett.*, **2001**, 173(1), 79–82.
- [17] Stearns M. E., Wang M., Type IV collagenase (M_r 72,000) expression in human prostate: benign and malignant tissue. *Cancer Res.*, **1993**, 53(4), 878–883.
- [18] Zheng H., Takahashi H., Murai Y., Cui Z., Nomoto K., Niwa H., Tsuneyama K., Takano Y., Expressions of MMP-2, MMP-9 and VEGF are closely linked to growth, invasion, metastasis and angiogenesis of gastric carcinoma. *Anticancer Res.*, **2006**, 26(5A), 3579–3583.
- [19] Zhou W., Yu X., Sun S., Zhang X., Yang W., Zhang J., Zhang X., Jiang Z., Increased expression of MMP-2 and MMP-9 indicates poor prognosis in glioma recurrence. *Biomed. Pharmacother.*, **2019**, 118, 109369.
- [20] Penning T. D., Talley J. J., Bertenshaw S. R., Carter J. S., Collins P. W., Docter S., Graneto M. J., Lee L. F., Malecha J. W., Miyashiro J. M., Rogers R. S., Rogier D. J., Yu S. S., Anderson G. D., Burton E. G., Cogburn J. N., Gregory S. A., Koboldt C. M., Perkins W. E., Seibert K., Veenhuizen A. W., Zhang Y. Y., Isakson P. C., Synthesis and Biological Evaluation of the 1,5-Diarylpyrazole Class of Cyclooxygenase-2

- Inhibitors: Identification of 4-[5-(4-Methylphenyl)-3-(trifluoromethyl)-1H-pyrazol-1-yl]benzenesulfonamide (SC-58635, Celecoxib). *J. Med. Chem.*, **1997**, *40*(9), 1347–1365.
- [21] Wolfe M. M., Lichtenstein D. R., Singh G., Gastrointestinal toxicity of nonsteroidal antiinflammatory drugs. *N. Engl. J. Med.*, **1999**, *340*(24), 1888–1899.
- [22] Liu C. H., Bao H. G., Ge Y. L., Wang S. K., Shen Y., Xu L., Celecoxib inhibits insulin-like growth factor 1 induced growth and invasion in non-small cell lung cancer. *Oncol. Lett.*, **2013**, *5*(6), 1943–1947.
- [23] Liu X., Wu Y., Zhou Z., Huang M., Deng W., Wang Y., Zhou X., Chen L., Li Y., Zeng T., Wang G., Fu B., Celecoxib inhibits the epithelial-to-mesenchymal transition in bladder cancer via the miRNA-145/TGFBR2/Smad3 axis. *Int. J. Mol. Med.*, **2019**, *44*(2), 683–693.
- [24] Dai H., Zhang S., Ma R., Pan L., Celecoxib inhibits hepatocellular carcinoma cell growth and migration by targeting PNO1. *Med. Sci. Monit.*, **2019**, *25*, 7351–7360.
- [25] Li J., Hao Q., Cao W., Vadgama J. V., Wu Y., Celecoxib in breast cancer prevention and therapy. *Cancer Manag. Res.*, **2018**, *10*, 4653–4667.
- [26] Saxena P., Sharma P. K., Purohit P., A journey of celecoxib from pain to cancer. *Prostaglandins Other Lipid Mediat.*, **2020**, *147*, 106379.
- [27] Liu B., Wen J. K., Li B. H., Fang X. M., Wang J. J., Zhang Y. P., Shi C. J., Zhang D. Q., Han M., Celecoxib and acetylbritannilactone interact synergistically to suppress breast cancer cell growth via COX-2-dependent and -independent mechanisms. *Cell Death Dis.*, **2011**, *2*(7), e185.
- [28] Zhou X., Shi X., Ren K., Fan G. T., Wu S. J., Zhao J.N., Celecoxib inhibits cell growth and modulates the expression of matrix metalloproteinases in human osteosarcoma MG-63 cell line. *Eur. Rev. Med. Pharmacol. Sci.*, **2015**, *19*(21), 4087–4097.
- [29] Zhang X., Chen J., Cheng C., Li P., Cai F., Xu H., Lu Y., Cao N., Liu J., Wang J., Hua Z. C., Zhuang H., Aspirin potentiates celecoxib-induced growth inhibition and apoptosis in human non-small cell lung cancer by targeting GRP78 activity. *Ther. Adv. Med. Oncol.*, **2020**, *12*, 1758835920947976.
- [30] Yamada K. M., Cell biology: tumour jailbreak. *Nature*, **2003**, *424*, 889–890.